Effect of Punch Profile Radius on Spring-back in V-bending of High Strength Steel and its FEA Simulation

By

PARVEEN KUMAR (08/PRD/2K10)

UNDER THE GUIDANCE OF Shri. **VIJAY GAUTAM** (Asst. Professor)

Submitted in partial fulfillment of the requirement for the award of the degree of

MASTER OF TECHNOLOGY

DEPARTMENT OF MECHANICAL ENGINEERING

DELHI TECHNOLOGICAL UNIVERSITY

DELHI TECHNOLOGICAL UNIVERSITY

FORMELY DELHI COLLEGE OF ENGINEERING

DELHI-110042

SESSION: 2010-2012

ABSTRACT

Spring-back is a common phenomenon in sheet metal forming, caused by the elastic redistribution of the internal stresses during unloading. It has been recognized that spring-back is essential for the design of tools used in sheet metal forming operations. A finite element (FE) program has been used to analyze the sheet metals axisymmetric V-bending process. [1].Numerical models by FEM were developed by using ABAQUS and DEFORM software. The principal objective of this analysis consists of predicting the spring-back for flanging and compares these results with some experimental data. [2] .Knowing that spring-back amount of bending material in bending dies is as important as the die itself, because the material leaving the die should be within the allowed tolerance limits. Therefore, in this study the subject of bending dies and spring-back in bending process has been researched. In order to find spring-back in bending, a ‘‘V’’ shaped die is designed and it has been aimed to find out how much can steel sheet metal materials resile in various angles and to bring forward spring-back graphics to add literature. There is little satisfying information in the literature regarding this issue.

In order to reach a conclusion, 6 different dies have been prepared, more than 54 samples, each of which have been bent and the obtained angles have been measured with profile meter. The acquired results have been statistically evaluated in a computer media and converted to graphics.

ACKNOWLEDGEMENT

I am grateful to **Prof. B.D Pathak**, Head Of Department (Production & Industrial Engineering) for giving me an opportunity to work with **Shri. VijayGautam**. I also expresses thanks to the lab staff to the lab staff at Mechanical Engineering Department, Delhi college of Engineering for providing me with the requisite resources.

I would like to express my deep sense of gratitude to **Shri. Vijay Gautam** for providing me with his invaluable guidance and support throughout the course of this project, and asking me accomplish my goals in this project. I also sincerely acknowledge the help of all people who directly or indirectly helped me in my project work and constantly encouraged me.

PARVEEN KUMAR (08/PRD/2K10)

CERTIFICATE

I hereby certify that the work which is being presented in the thesis entitled “Effect of Punch Profile Radius on Spring-back in V-bending of High Strength Steel and its FEA Simulation” in the partial fulfillment of requirement for the award of degree of **MASTER OF TECHNOLOGY** at **DELHI COLLEGE OF ENGINEERING** under **DELHI TECHNOLOGICAL UNIVERSITY, DELHI,** is an authenticated record of following student **PARVEEN KUMAR** submitted in the Department of Mechanical Engineering carried out during 4^{th}semester, under my supervision.

PROJECT SUPERVISOR:

Shri Vijay Gautam

Department Of Mechanical Engineering

Delhi Technological University

TABLE OF CONTENTS

Chapter 3

METHODOLOGY

Chapter 4

Code development and their validation

LIST OF SYMBOLS

α = is the bend angle (in radians)

R = bend radius

t = sheet thickness

K = location of neutral axis from bottom surface

e_o=strains the outer fibers

e_i =strains inner fibers

R_B =forming radius

W = width of the die opening

F_{max} =maximum bending force

UTS = ultimate tensile strength

L =length of the part

R_I =bend radius before spring back

R_F=bend radius after spring back

K_s = spring-back ratio

α_i = bending angle before springback

α_f =bending angle after springback

z = the distance of an element from neutral axis in the bend region

α= bend angle

L_0 = Arc length at the mid-plane

e= engineering strain

ε_x = true strain in x-axis

εy =true strain in y-axis

ε_z, =true strain in z-axis

Fx =net external force

M= bending moment

σ_x=stress in x direction

S=plane strain yield stress

E' =Modulus of elasticity in plane strain

ν= Poisson's ratio.

E= uniaxial Young's modulus

Y= distance from middle surface to stress at some distance

ρ = radius of curvature of *sheet* of a cylindrical bent region

σ= representative/effective or equivalent stress,

K' =strength coefficient

$\epsilon_w = \mathrm{straininwidthdirection}$

$\epsilon_t = \mathrm{straininthicknessdirection}$

$R_p =$ Plastic strain ratio

List of Figures

List of Tables

CHAPTER 1

INTRODUCTION

Sheet metal is a critical material for vehicle design due to design versality and manufacturability. Low carbon steel sheet has long been the workhorse material in auto and consumer industries it can be stamped into inexpensive, complex components at very high production rates.

1.1 SHEET METAL FORMING OPERATIONS

In sheet metal forming a shape in produced from a flat blank by stretching and shrinking the dimensions of all its volume elements in three mutually perpendicular principal directions. A large variety of shapes such as singly curved parts, contoured flanged parts, curved sections, deep recessed drawing parts, etc.

1.2 BENDING OF SHEET METAL

Bending is one of the most important sheet metal forming operations by which a straight length is transformed into a curved one with the help of suitably designed die and punch. It is very common process of changing sheet and plate into channel, drums, tanks, car bodies, aircraft fuselages etc. In addition is a part of deformation in many other forming process.

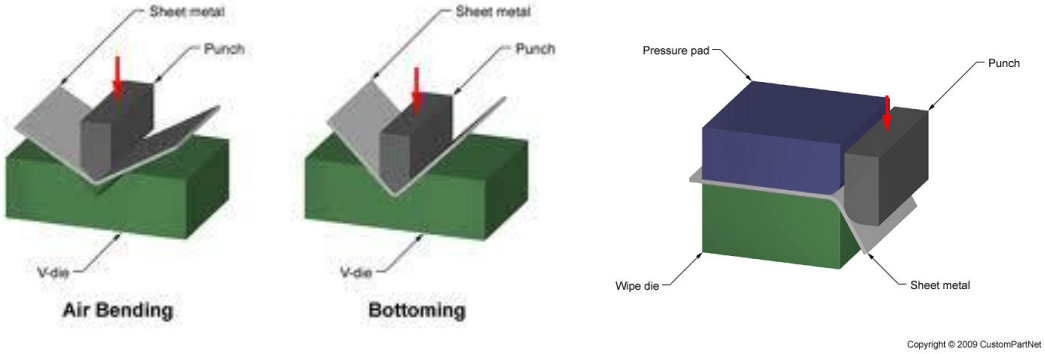

(a)V-Bending Operation (b) Wipe Bending Operation

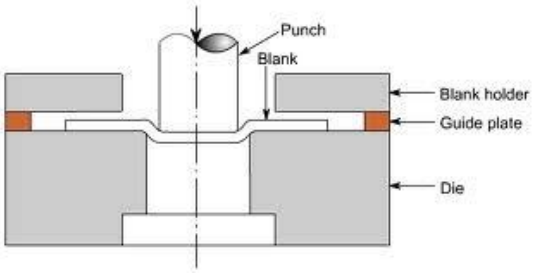

Figure 1.1: Various Bending Operations [8]

Other Bending Operations

- U – Bending
- Air Bending
- Offset Bending
- Hemming
- Seaming
- Curling
- Channel
- Flanging
- Corrugating
- Tube Forming

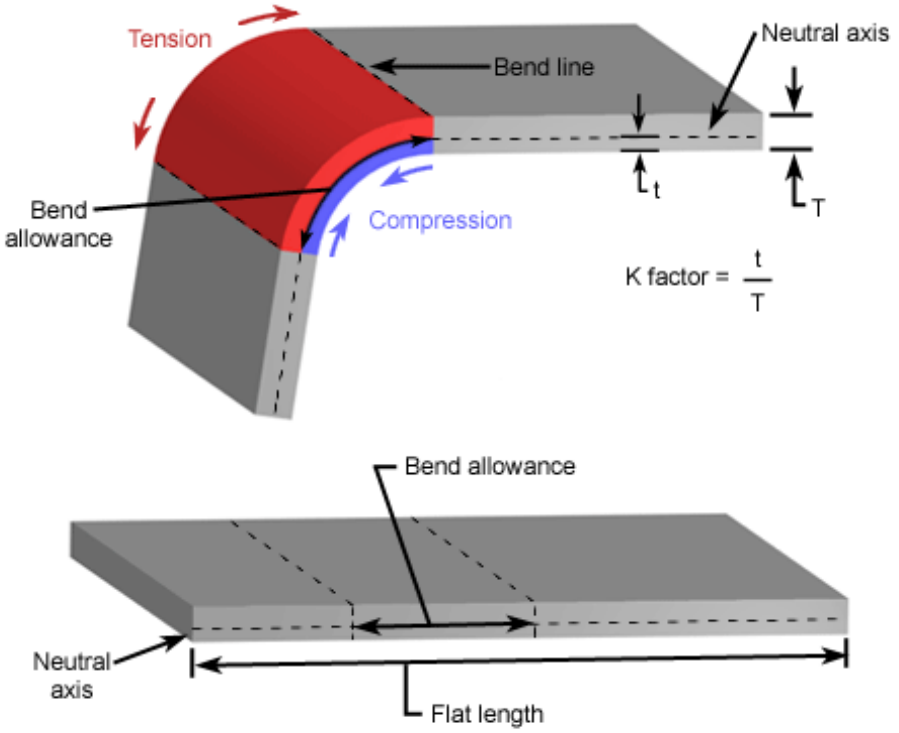

Figure 1.2: Bending Geometry

Bend Allowance is the length of Neutral Axis in the Bend Area and is used to determine the blank length for a bent part. However the radial position of the neutral axis depends on the bend radius and bend angle, an approximate formula for the bend allowance is α(R+kt).

Where,α is the bend angle(in radians),R is the bend radius, k is constant, and t is the sheet thickness. For an ideal case the neutral axis remains at the center and hence k=0.5, value of k varies from 0.33 to 0.5.

Minimum bend radius: The outer fibers of the part being in tension, and the inner fibers are in compression. Theoretically the strains at the outer and inner fibers are equal in magnitude and are given by

$$e_o = e_i = 1/(2R/t) + 1 \qquad (1.1)$$

However due to shifting of neutral axis towards the inner surface, the length of the bend is smaller in the outer region than in the inner region. Consequently the outer and inner strains are different and the difference increases with decreasing R/t ratio. The radius R at which a crack appears on the outer surface of the bend is called minimum bend radius.

1.3 STRESSES IN BENDING

During bending, the entire stress-strain curve in traversed. Only the natural line retains its original length. As shown in figure 1.2 , fibers below the neutral line are subjected to tensile (+) stress and fibers above the natural line are subjected to compressive (-) stress. Stresses are greatest on the outside and zero at neutral line. For a given sheet thickness T, tensile and compressive strains increase with decrease with decreasing forming radius Rb (i.e. with decreasing R_b/T

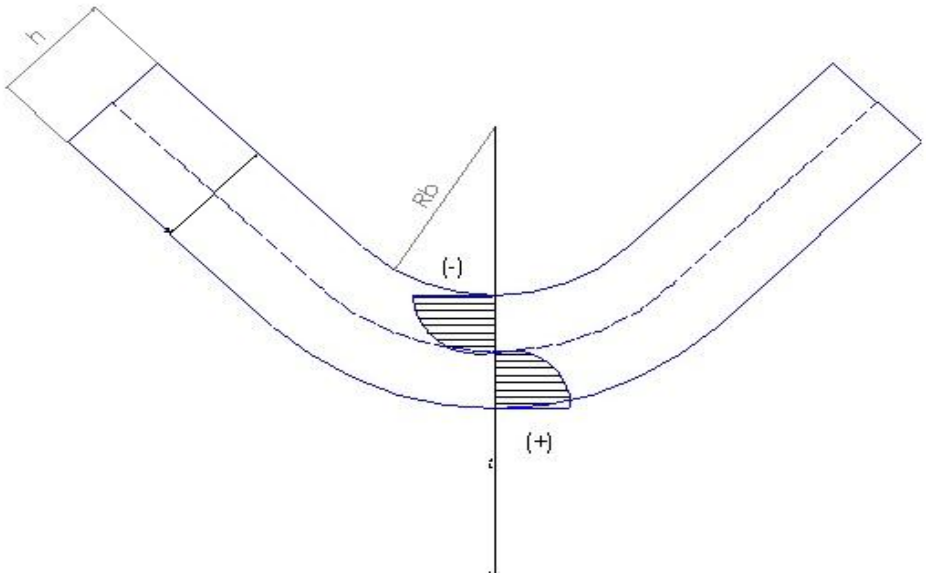

Figure 1.3: Stresses in Bending

Bending Forces can be estimated by assuming that the process is that of the simple bending of rectangular beam. Thus, the bending force is a function of the strength of material, the length and thickness of part, and the width Wof the die opening, excluding friction, the general expression for the maximum bending force is

$$F_{max} = k\ UTS \frac{Lt^2}{W} \quad (1.2)$$

Where k ranges from 1.2 to1.33 for a V-die, the k values for wiping and U dies are 0.25 and 2 times respectively that for V dies. The effect of various factors such as friction, on the bending force, is included in factor k.

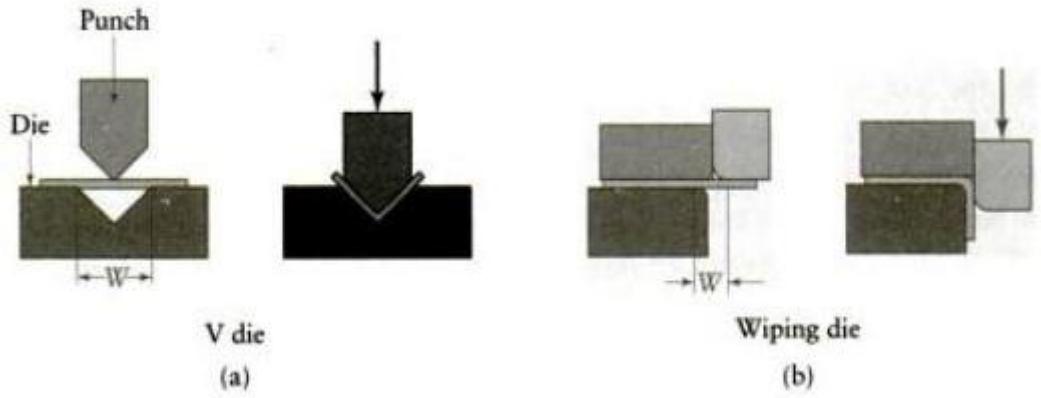

FIGURE 1.4: Various types of bending [REF 5: Manufacturing process for Engineering Materials ,KALPAKJIAN,Serope]

The bending force is also a function of punch travel, it increases from zero to maximum and may decrease as the bends completed. The force then increases sharply as the punch bottoms in case of die bending.

1.4 SPRINGBACK

The stress state is complex in bending. Around the neutral plane, the stress must be elastic because complete tensile and compressive stress-strain curves of the material are traversed on both bend side. When the forming tool is removed from the metal, the elastic components of stress cause spring back which changes both the angle and radius of the bent part as shown in Figure 1.4. The part tends to recover elastically after bending, and its bend radius becomes larger. This elastically-driven change in shape of a part upon unloading after forming is referred to as spring back.

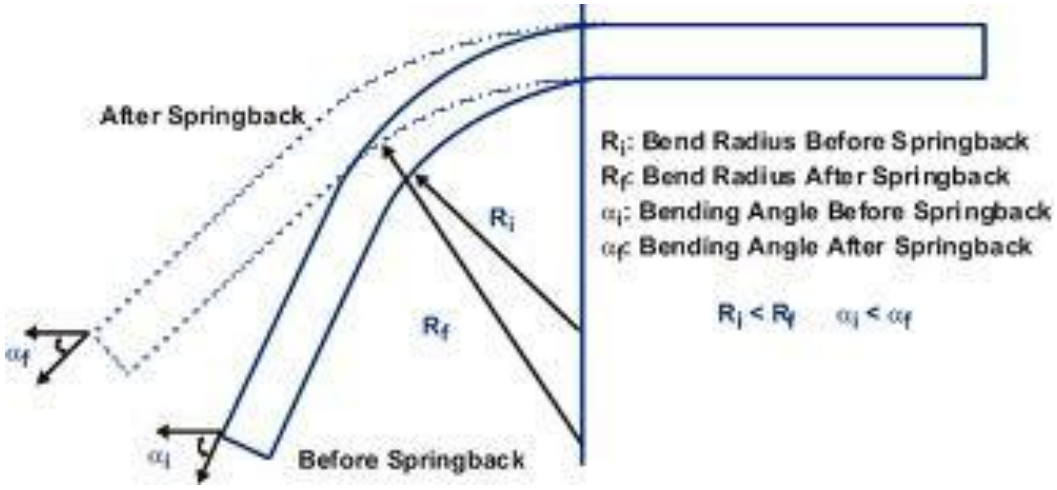

Figure 1.5 Spring-back Phenomenon in bending [REF: Manufacturing process for Engineering Materials ,KALPAKJIAN,Serope]

Spring-back poses a major problem in sheet bending operation as it cause a shape change that makes the assembly of the parts very difficult and its compensations are to be taken care of while designing the dies and punches.

The spring-back is measured in terms of the ration of initial and the final angle of the sheet, called as spring-back ratio (K_s).

$$K_s = \alpha_f - \alpha_i \quad (1.3)$$

Spring-back establishes new force equilibrium with a residual stress distribution typified by a compressive stress on the outer and tensile stress on the inner surface.

1.4.1 COMPENSATION OF SPRINGBACK

Spring-back may be reduced by:

- Over-bending[figure 1.6(a),(b)]
- Plastic deformation at the end of the stroke, and[Figure 1.6(c)]
- Subjecting the bend zone to compression during bending with a counterpunching Coining Process[Figure 1.6(d)]

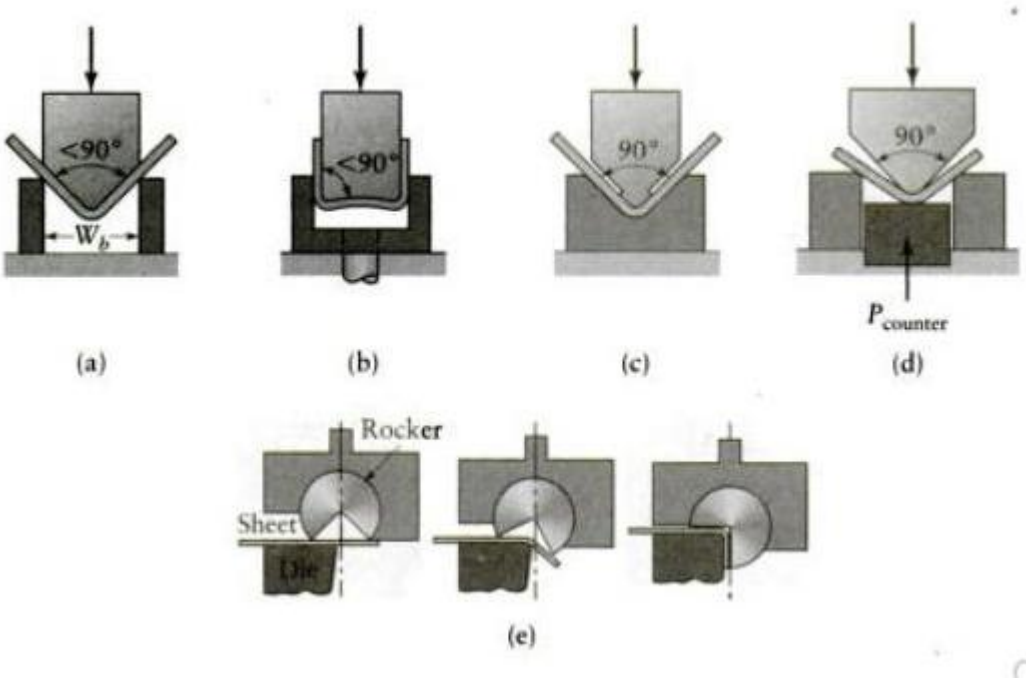

Figure 1.6: Spring-back compensation methods

1.5 MOTIVATION AND PROBLEM DEFINITION

Spring-back is a common phenomenon in sheet metal forming, caused by the elastic redistribution of the internal stresses during unloading. It has been recognized that spring-back is essential for the design of tools used in sheet metal forming operations.

Recently, in automotive industry many companies, abroad, are trying to form the body panels in single stamping operation while keeping the material costs and the crap down by using IFHS blanks. The push for usage of IFHS in the auto industry results from the need of fuel conservation, safety mandate, customer demands, and environmental concerns to design lighter automobiles that are more fuel efficient, produce lower emissions, with improved handling and overall improvement of structure the vehicle.

Spring-back causes following problems in sheet-metal forming:

1) The assembly of the sheet metal components becomes problematic thereby increasing the assembly time and reducing the productivity.
2) Rolling direction affects the spring-back as the strength of the sheet-metal is different in different directions i.e. IFHS sheet metal is anisotropic.
3) In automobile industry different punch corner radius are used for different bending operations which in turn affects the spring-back in components.
4) A wide range of thickness is used in sheet-metal components which again affects the spring-back.
5) High strength sheets are preferred for automotive body as to reduce the thickness which results in reduction of the overall weight of the vehicle. Lighter vehicles are in demand for higher fuel efficiency.

However, spring-back characteristic of IFHS has not been investigated widely and very little information is available about its behavior during bending operations.

1.6 OBJECTIVES

In the view of above mentioned facts the spring-back has been analyzed in V-bending process with the following objectives:

1. To determine the effect of punch corner radius on spring-back of IFHS steel sheet with reference to the rolling direction (i.e. 0˚, 45˚, and 90˚)and to include the effects of anisotropy of sheet metal in V-bending operation.
2. To determine the effect of thickness on spring-back of sheet metal (i.e. 0.9mm. 1.2mm and 1.6mm) in V Bending.
3. Simulation of V-bending process using FEA to predict the spring-back in the above cases.
4. Validation of experimental results with FEA results.
5. To suggest a model to compensate the spring-back in v- bending process.

CHAPTER 2

LITERATURE REVIEW

Bending of sheet metal is important manufacturing process. Large number of studies has been carried out to gain a deep understanding of this process. A brief summary of the available literature on various aspects of sheet bending is given below:

2.1 INTERNATIONAL STATUS

2.1.1 BENDING THEORIES

Hill (1950) presented a complete solution for pure bending in which deformation of sheet metal is achieved by a couple applied along its length. In the analysis, hill predicted the movement of neutral surface but no change in the thickness for rigid perfectly materials under plane strain bending.

Lubahn and **Sachs** (1951) analyzed, in a manner similar to hill's , the bending of rigid perfectly plastic materials in cases of both plane stress and plane strain , and they predicted no change in material thickness by assuming that the surfaces, including the neutral surface, **Crafoord**(2001) considered the Bauschinger effect by assuming the constant yield surface on reverse straining by fibers overtaken by the neutral surface. And he predicted obvious thickness thinning of rigid-strain-hardening metal sheets.

Dadras and **Majlessi**(1982) conducted an analysis on plane strain plastic bending of rigid –work hardening materials and they proposed two models. In model 1, a numerical solution based on a linear "sigma"-epsilon" approximation for fibers in reversed loading has been presented. Model 2 is an extension of proksa's analysis

to the case of materials described by **ludwik's** equation. It has been demonstrated that the result of these models are generated in close agreement.

The difference between all these theories of pure bending was in choosing the strain hardening models or considering Bauschinger effect.

2.1.2 GENERALIZED BENDING THEORY [Hosford(1993), Duncan(2002)]

Figure 2.1shows the coordinate system. Let r be the radius of curvature measured at the mid-plane and let z be the distance of an element from the mid-plane. The engineering strain at z can be derived by considering the arc length L, measured parallel to the surfaces of the sheet in the x-direction. The arc length at the mid-plane, L_0, doesn't change during bending and may be expressed as L_0= r α, where $\alpha$is the bend angle. At z, the arc length is L = (r + z) α. Before bending, both arc lengths were equal so the engineering strain, e, is

$$\mathrm{ex} = \frac{L - L0}{L0} = \frac{z\alpha}{r\alpha} = \frac{z}{r}. \qquad (2.1)$$

The true strain, ε_x, is

$$\boldsymbol{\varepsilon}_x = \ln\left(1 + \frac{z}{r}\right) \qquad (2.2)$$

For many bends the strains are low enough so we can approximate

$$\boldsymbol{\varepsilon}\mathrm{x} = \frac{\mathrm{z}}{\mathrm{r}} \qquad (2.3)$$

With wide sheets (w>>t) the width strain, εy, is negligible. Therefore sheet bending can be considered to be a plane-strain operation, $\varepsilon_z = -\varepsilon x$. The value of ex varies from −t/(2r) on the inside (z = −t/2) to zero at the mid-plane and +t/(2r) on the outside surface. For small strains, $\varepsilon x \approx e_x$. The internal stress distribution can be found from the strain distribution and the stress–strain curve.

Assuming that the material is elastic - ideally plastic (no strain hardening). Let the tensile yield strength in plane strain be Y.

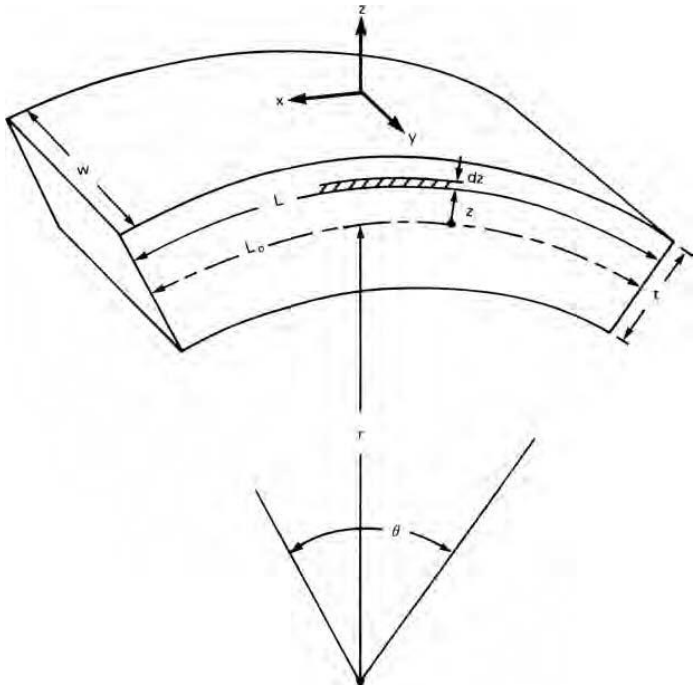

Figure 2.1: Coordinate system for analyzing sheet bending

Figure 2.2: Shows the strain and stress distribution. The entire cross section will at a stress $\sigma_x = Y$ or $-Y$ except for an elastic core near the mid-plane. For most bending operations this elastic core can be neglected. The bending moment can be calculated assuming that there is no net external force, Fx.

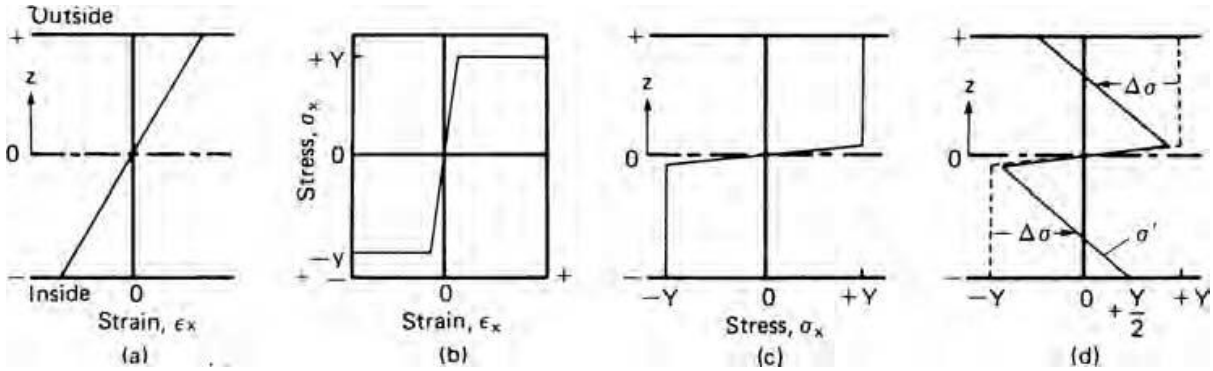

Figure 2.2. Stress and strain distribution across a sheet thickness. During bending the strain varies linearly across section (a). With a non–strain-hardening material (b) the bending causes the stress distribution in (c). Elastic unloading results in the residual stresses in (d).

However, there are internal forces, dFx= σ_xw dz, acting on incremental elements of the cross section. The contribution of stress on every element to the bending moment is the product of this incremental force times its lever arm, so dM= zσ_xw dz. The total bending moment is then

$$M = \int_{-\frac{t}{2}}^{+\frac{t}{2}} w\sigma xz\, dz = 2\int_{0}^{\frac{t}{2}} w\sigma xz\, dz \qquad (2.4)$$

It is simpler to take twice the integral between 0 and t/2 because the sign of σx changes at the mid-plane. For an ideally plastic material

$$M = 2w\int_{0}^{\frac{t}{2}} z\ dz = \frac{Yt^2}{4} \qquad (2.5)$$

2.1.3Elastic, perfectly plastic model

If the bend ratio is not less than about 50, strain-hardening may not be so important and the material model can be that shown in Figure 2.3(b).

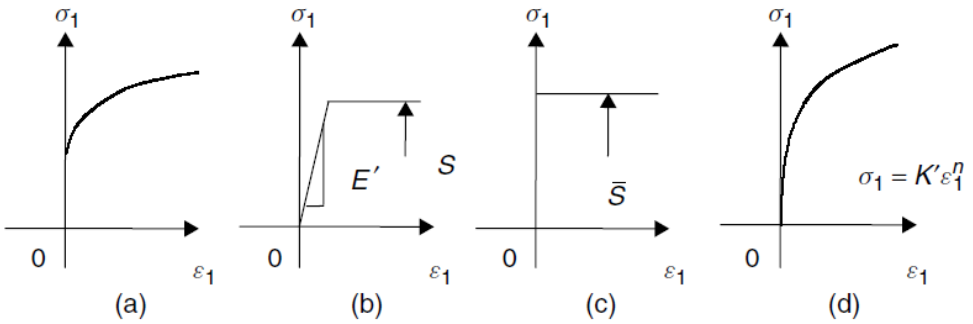

Figure 2.3: Material models for bending. (a) An actual stress–strain curve. (b) An elastic, perfectly plastic model. (c) A rigid, perfectly plastic model. (d) A strain-hardening plastic models less than the plane strain yield stress, *S*

$$\sigma 1 = E'\varepsilon 1 \qquad (2.6)$$

Where the modulus of elasticity in plane strain is slightly different from the uniaxial Young's modulus, E i.e.

$$E' = \frac{E}{1-\nu^2} \qquad (2.7)$$

Where$\nu$is Poisson's ratio.

For strains greater than the yield strain,

$$\sigma 1 = S$$

where S is constant.

2.1.4 Strain-hardening model

Where the strains are large, the elastic strains may be neglected and the power law strain hardening model used, where

$$\sigma_1 = K'\epsilon_1^n \quad (2.8)$$

For a material having a known effective stress–strain curve of the form

$$\bar{\sigma} = \epsilon_f = K\bar{\epsilon}^n$$

2.1.5Bending of a strain-hardening sheet

If a power law strain-hardening model of the kind shown in Section 2.1.5 and Figure 2.2(d) is used. The whole section is assumed to be deforming plastically and the stress at some distance, *y*, from the middle surface is

$$\sigma_1 = K'\epsilon_1^n \approx K'\left(\frac{y}{\rho}\right)^n$$

The equilibrium equation can be written as

$$M = 2K'\left(\frac{1}{\rho}\right)^n \int_0^{\frac{t}{2}} y^{1+n}\, dy = K'\left(\frac{1}{\rho}\right)^n \frac{t^{n+2}}{(n+2)2^{n+1}} \quad (2.9)$$

These equations can be combined to give a set of equations for bending a non-linear Material, i.e.

$$\frac{M}{I_n} = \frac{\sigma_1}{y_n} = K'\left(\frac{1}{\rho}\right)^n$$

Where

$$I_n = \frac{t^{n+2}}{2^{n+1}(n+2)} \quad (2.10)$$

2.1.6IMPORTANT FACTORS IN BENDING

A) DESIGN PARAMETERS:

The critical design parameters in sheet metal forming operations include the die corner radius, punch corner/nose radius clearance punch and die etc.

B) SHEET METAL PROPERTIES:

Most polycrystalline materials possess a texture (directional properties) are determined in tension tests. Which are repeated in the different directions relative to the rolling direction.

Plastic strain ratio: this ration is measure of anisotropy and its value indicated the resistance of a materials to thinning (Hosford(1993))

$R_p = \epsilon_w / \epsilon_t$

Where,

$\epsilon_w = strain\ in\ width\ direction$

$\epsilon_t = strain\ in\ thickness\ direction$

The anisotropy is of two types:

1). Normal anisotropy,

$$\bar{R} = \frac{[R_0 + R_{45} + R_{90}]}{4} \qquad (2.11)$$

2). Planar anisotropy

$$\Delta R = \frac{[R_0 - 2R_{45} + R_{90}]}{2} \qquad (2.12)$$

The R value with subscript denotes the value for specimen taken at that angle to the rolling direction.

Tan et al. (1995) studied the effect of anisotropy on pure bending of sheet metals. They proposed two models one neglecting the Bauschinger effect and the other considering the Bauschinger effect. They also found that the effect of anisotropy on material thinning of bend is small but has a relatively large effect on the bending moment.

A rigorous solution for the elastic – plastic bending of wide sheets exhibiting normal anisotropy has been presented by chakra arty el al .(2001) assuming a state of plane strain for deformation mode . Such a solution is necessary for a critical evaluation of elementary theories of sheet bending in the partially plastic stare. The results indicated that the elementary bending theory significantly overestimates the magnitude of the bending couple to produce a given elastic – plastic curvature of the bent sheet.

2.1.7SPRINGBACK IN SHEET METAL BENDING

In the bending processes, when the forming forces have been removed, the metal tries to return to its original shape and results in a phenomenon called ‘’spring-back’’.

Spring-back is a function of both the material properties and die configuration: the greater the strength and lower the elastic modulus of the material, and the larger the bend radius and die gap, the greater the spring back will be.

The spring-back was addressed by Gardiner (1957), who proposed a mathematical formula for spring-back calculations based on elementary bending theory with ideal plasticity.

Johnson and Yu(1981) further developed Gardiner's work for linearly hardening materials for bending with tension.

Ferreira et al.proposed a method to automatically measure the spring-back angles by using computer vision and digital image processing techniques.

Sun et al.proposed a method of evaluating spring-back in sheet metal formed on a hydraulic press in real time.

Tekaslan et al.examined spring-back of 0.5 mm steel sheet metal in V-bending dies using four different methods.

Li et al.(2002) found that the material's hardening model directly affects the accuracy of spring-back calculation. The greater the accuracy of the hardening model, the greater the spring accuracy. The spring-back calculated with the elasto-plactic power-exponent hardening model agrees better with experimental result than that calculated with the linear-hardening model.

2.1.8 GENERAL ASPECTS OF SPRINGBACK

Elastic unloading and spring-back

If a sheet is bent by a moment to a particular curvature, and the moment then released, there will be a change in curvature and bend angle. The length of the mid-surface is

$$l = \rho\theta$$

This will remain unchanged during unloading as the stress and strain at the middle surface are zero. From this, we obtain

$$\theta = l\frac{1}{\rho} \qquad (2.13)$$

Differentiating Equation 2.13, in which *l* = constant, we obtain

$$\frac{\Delta\theta}{\theta} = \frac{\Delta\left(\frac{1}{\rho}\right)}{\frac{1}{\rho}} \qquad (2.14)$$

Spring-back in an elastic, perfectly plastic material

The assumed stress–strain curve for an elastic, perfectly plastic material that undergoes reverse loading. (This neglects any Bauschinger effect; this is the phenomenon of softening on reverse loading that is observed in many materials.). A change in stress of $\sigma 1 = -2S$ can occur without the material becoming plastic. If we assume that the unloading of the sheet will be an elastic process, then the elastic bending equations, Equations, can be written in difference form, i.e.

$$\frac{\Delta M}{I} = \frac{\Delta\sigma_1}{y} = \frac{\Delta\sigma_{1max}}{\frac{t}{2}} = E'\Delta\left(\frac{1}{\rho}\right) \quad (2.15)$$

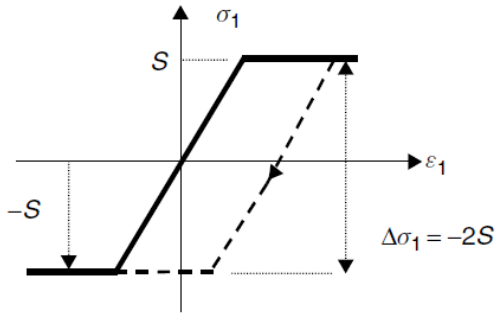

Figure 2.4:Elastic, perfectly plastic material model with reverse loading.

For a sheet that has been bent to the fully plastic moment, the unloading curve will be parallel to the elastic loading line.

we see that for a change in moment of −*M*p,

$$\frac{\Delta\left(\frac{1}{\rho}\right)}{\left(\frac{1}{\rho}\right)_e} = \frac{\Delta M}{M_e} = -\frac{M_p}{M_e} \quad (2.16)$$

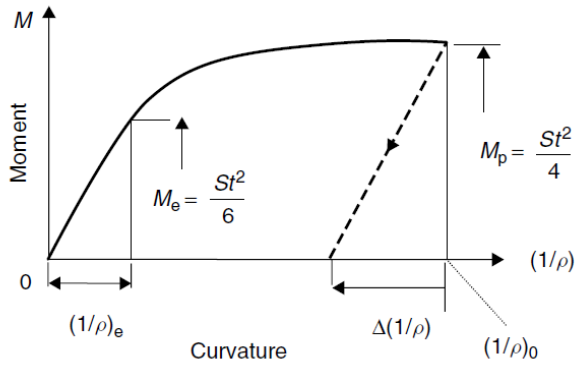

Figure 2.5: Moment, curvature diagram for an elastic, perfectly plastic sheet showing unloading from a fully plastic moment.

The ratio of the fully plastic moment to the limiting elastic moment has been shown to be

$$\frac{M_p}{M_e} = \frac{3}{2}$$

Therefore,

$$\Delta\left(\frac{1}{\rho}\right) = -\frac{3}{2\left(\frac{1}{\rho}\right)_e} = -\frac{3S}{E't} \qquad (2.17)$$

If the sheet has been unloaded from a curvature of *(1/ρ)*0, the proportional change in curvature, from Equation 2.17 is

$$\frac{\Delta\left(\frac{1}{\rho}\right)}{\left(\frac{1}{\rho}\right)_e} = -\frac{3S\rho_o}{E't} \qquad (2.18)$$

Or, from Equation 2.18, the change in bend angle is

$$\Delta\theta \approx -\frac{3S\rho_o\theta}{E't} \qquad (2.19)$$

Equation 2.19 is only approximate and applies to small differences in angle or curvature and to the case in which the sheet has been bent to a nearly fully plastic state.

Nevertheless, the equation is very useful and indicates that spring-back is proportional to:

- The ratio of flow stress to elastic modulus, *S/E'*, which is small and often of the order of 1/1000;
- The bend ratio ρ_0/t;
- The bend angle.

Thus spring-back will be large when thin high strength sheet is bent to a gentle curvature.

Residual stresses after unloading

When an elastic, perfectly plastic sheet is unloaded from a fully plastic state, it is shown

above that the change in moment is _*M* = −*M*p. Substituting in Equation 2.15

$$-\left(\frac{St^2}{4}\right)/(t^3/12) = \Delta\sigma_{1max}/(t/2) \qquad (2.20)$$

I.e. the change in stress at the outer fiber is

$$\Delta\sigma_1 = -\frac{3S}{2} \qquad (2.21)$$

(Equation 2.21 supports the assumption that for the simple bending model given here, the unloading process is fully elastic.)

Thus the effect of unloading is equivalent to adding an elastic stress distribution of maximum value of –3S/2 to the fully plastic stress state as shown in Figure 2.6. The residual stress distribution is shown on the right of Figure 2.6; this is an idealized representation arising from the simple model, but it does show that after unloading, the tension

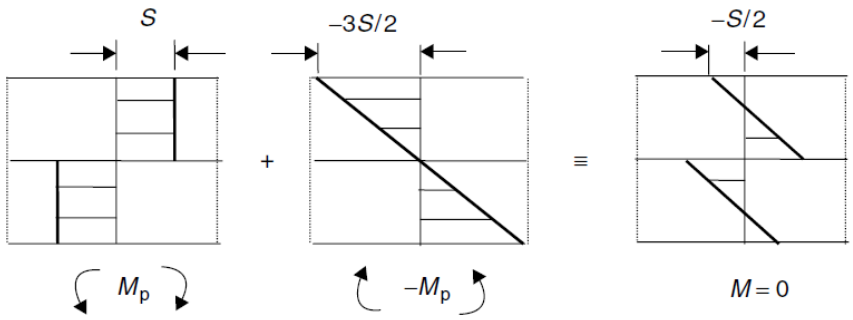

Figure 2.6:Residual stress distribution after unloading from a fully plastic moment.

side of the bend would have a significant compressive residual stress at the surface and there would be a residual tensile stress on the inner surface.

NEUTRAL AXIS SHIFT

The analyses above are based on the neutral plane remaining at the mid-plane of the sheet. Actually the neutral plane moves toward the inside of the bend. There are two reasons for this: On the inside of the bend, elements thicken. Also, the true compressive strains on the inside are greater in magnitude than the strains on the outside.

The thickness of element i is $t_i = t0/(1 + e_i) = t0/(1 + z_i/\boldsymbol{\rho})$ and the true strain, **ε**i, at element i is0ln(1+ zi /**ρ**).

If eiis positive, the true stress, $\boldsymbol{\sigma}_i$, on element i is $\boldsymbol{\sigma}i = K\boldsymbol{\varepsilon}_i^n = K[\ln(1 + zi/\boldsymbol{\rho})]n$. If ei is negative, the true stress, **σ**ion element is $\boldsymbol{\sigma}i = -K(\ln(1 + zi/\boldsymbol{\rho})|n$. The force on element i, on the tensile side of the bend is then

$$Fi = [wt0/(1+zi/\boldsymbol{\rho})]K[\ln(1+zi/\boldsymbol{\rho})]n$$

and on the compressive side

$$Fi = -[wt0/(1+zi/\boldsymbol{\rho})]K|\ln(1+zi/\boldsymbol{\rho})|n.$$

Wherez_i is negative on the inside of the bend and positive on the outside. The ratio of the two at equal displacements from the original centerline is

$$\frac{FO}{FI} = \frac{\left[\frac{ln\left(1+\frac{z_{iO}}{\rho}\right)}{ln\left(1+\frac{z_{iI}}{\rho}\right)}\right]^n \left(1+\frac{z_{iI}}{\rho}\right)}{1+\frac{z_{io}}{\rho}}, \qquad (2.22)$$

wherez_{iO} refers to an element on the outside of the bend and z_{il} refers to an elementon the inside of the bend.

2.1.10 FACTORS INFLUENCING SPRINGBACK

1. Young's modulus:

Spring reduces with increase in elastic modulus, because the resistance to elastic bending increases with increase in elastic modulus (Wang et al (1993))

2. Yield stress:

Spring-back increases with increase in yield stress, because higher the strength the more will be the resistance to plastic yielding.

3. Plastic anisotropic ratio(r) and hardening coefficient (n):

The higher the normal anisotropic values the more the spring-back was observed.

Dae (1997) developed an analytic model to predict the effect of normal anisotropy and hardening coefficient and arrived at the concluded that spring-back is almost proportional to the normal anisotropic parameter and decreases sharply with smaller strain hardening exponent n. And at higher values of n and thickness ratio, the change in spring-back values is very smaller. But this model ignored the variation of r in the plane strain of the sheet.

2.1.11 SPRINGBACK COMPENSATION METHODS

The purpose of these methods is to minimize the deviation of the produced part, shape from the tooling shape which is identical to the desired shape.

Rosochowski (2001) presented a method for spring-back compensation based on a hybrid physical modeling /finite element approach .physical modeling provides information on load distribution at the material/die interface which is then used as a load boundary condition in the two separate finite element simulations of die deflection and component spring-back. The die compensation part is carried out in a CAD environment.

Ayers(1984)has suggested the use of multi-step process to reduce spring-back while avoiding the part failure.

Liu(1988)has proposed variation of binder force during the forming process, thereby providing tensile preloading or post-loading on the formed part .In order to reduce spring-back in both of these methods the reduction of spring-back is effected by the provision of high amounts of stretching of the formed part.

Woo et al .(1959)and Wenner (1983)showed that the tensile stretching stresses superimposed on the bending stresses of an elastic-plastic material cause the reduction of spring-back in two dimensional formed parts. However Wenner(1983)also pointed out that it is not always possible to transmit high tensile forces to all parts of a work piece of a complicated geometry without causing failure by tearing of work piece.

CHAPTER 3

METHODOLOGY

In present study the spring-back of tailor welded strips has been analyzed in V-bending operation. The methodology includes experimental, analytical methods and finite element analysis.

3.1 SHEET MATERIAL FOR BENDING

The development of deep-draw able sheet steels is of particular significance for the automotive industry. Titanium and /or Niobium added extra-low carbon interstitial free (IF) steels are relatively new materials developed for critical applications in auto industry. In this study these extra low carbon steel of two different grades viz. IF (Interstitials-Free) and IFHS (Interstitials-Free High Strength) have been used to investigate the effect of different material properties on spring-back of Blank. The virtually complete removal of carbon and nitrogen in these materials leads to high formability and hence these are generally used in forming of complex parts. The chemical composition of IF and IFHS grades is reproduced here as reported by Singh (2005) and Panda (2006) are given in table 3.1

C	Si	Mn	P	S	Ti	Nb	Al
0.0027	0.013	0.4	0.05	0.011	0.04	0.001	0.032

Table 3.1: Chemical composition of IFHS-steel (wt %)

3.2MICROSTRUCTURE OF IFHS

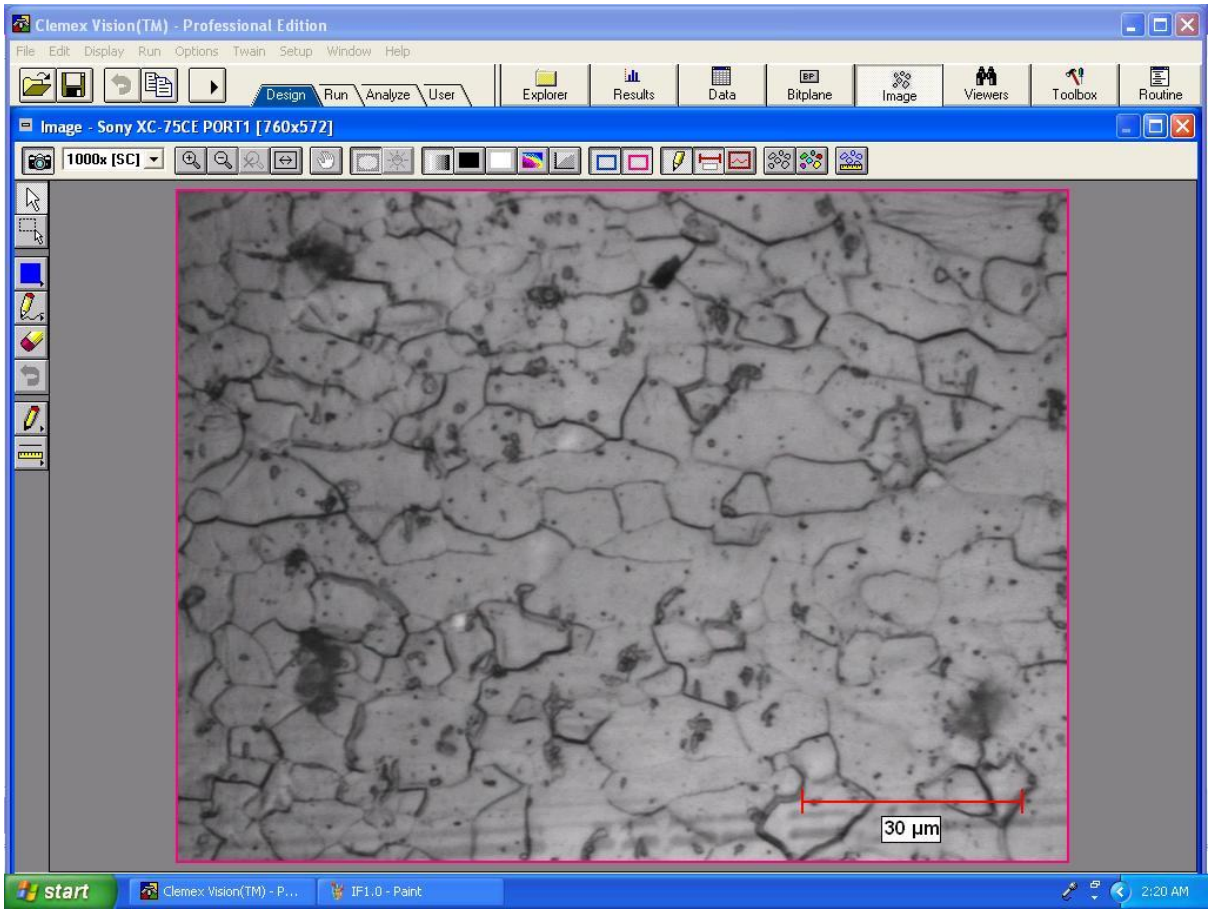

Fig3.1. Microstructure of IFHS at 1000x

3.3 TESTS FOR DETERMINATION OF MATERIAL PROPERTIES

The tension tests were carried out as per ASTM standard E 8M-04 (2004) on *INSTRON 5582, 100KN*machine, in strength of materials laboratory at IIT Delhi. The IFHS sheets of HF grade (0.9 mm, 1.2mm and 1.6 mm thickness) were tested for the mechanical properties. The tension test for material was carried out with standard size specimen as shown in Fig 3.4.

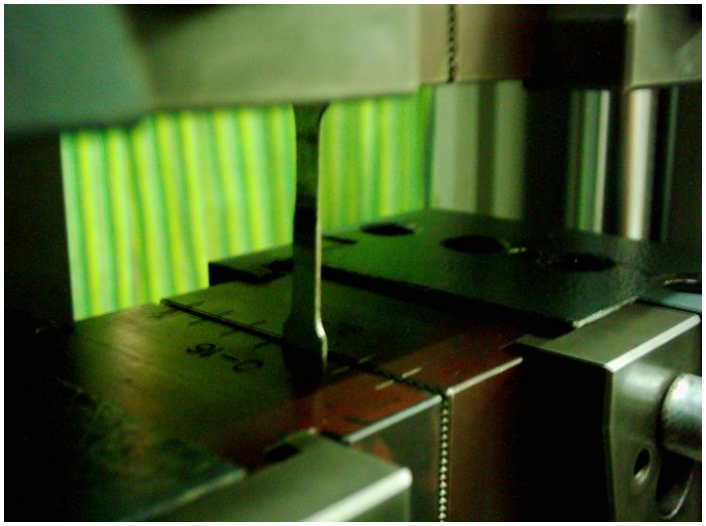

Figure 3.2: Tension test setup

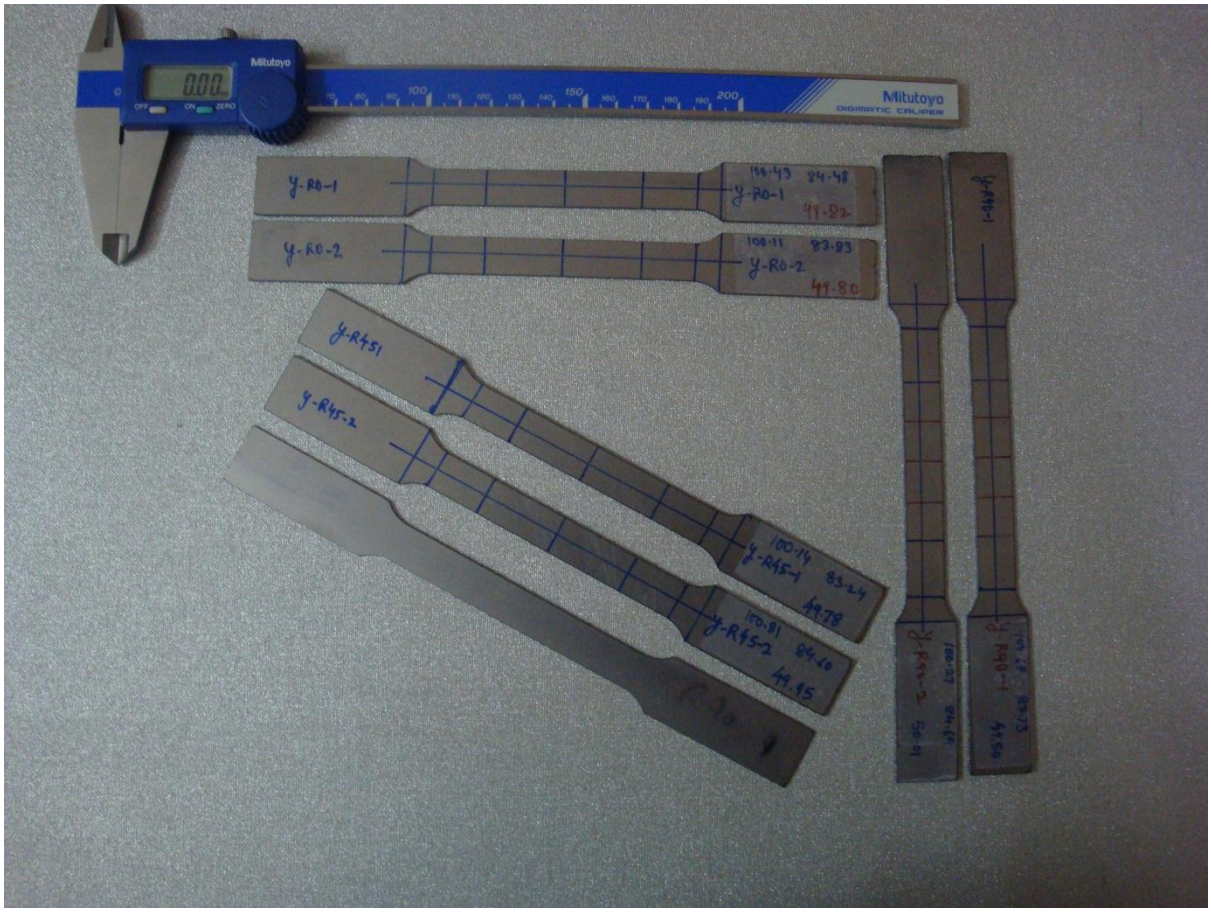

Fig 3.3. Specimen with rolling direction (i.e. 0˚, 45˚, 90˚)

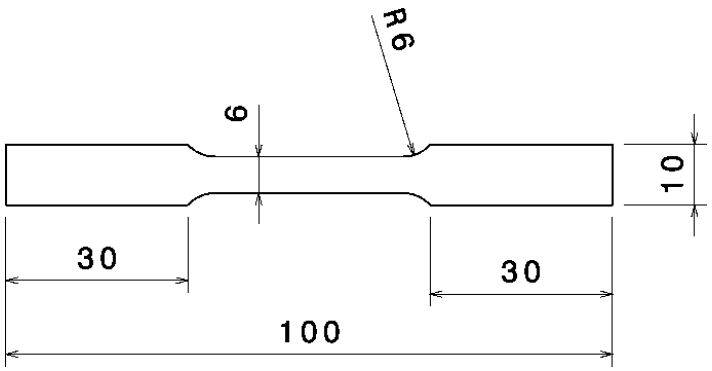

Fig 3.4. Specimen dimensions

3.3.1 Yield Stress and UTS

The typical stress strain curve obtained from the tests is shown in Figure 3.7 and Figure 3.8. Since the departure from the linear elastic region cannot be easily identified, the yield stress was obtained using the 0.2 % offset method. UTS was determined for the maximum load and original cross section area of specimen.

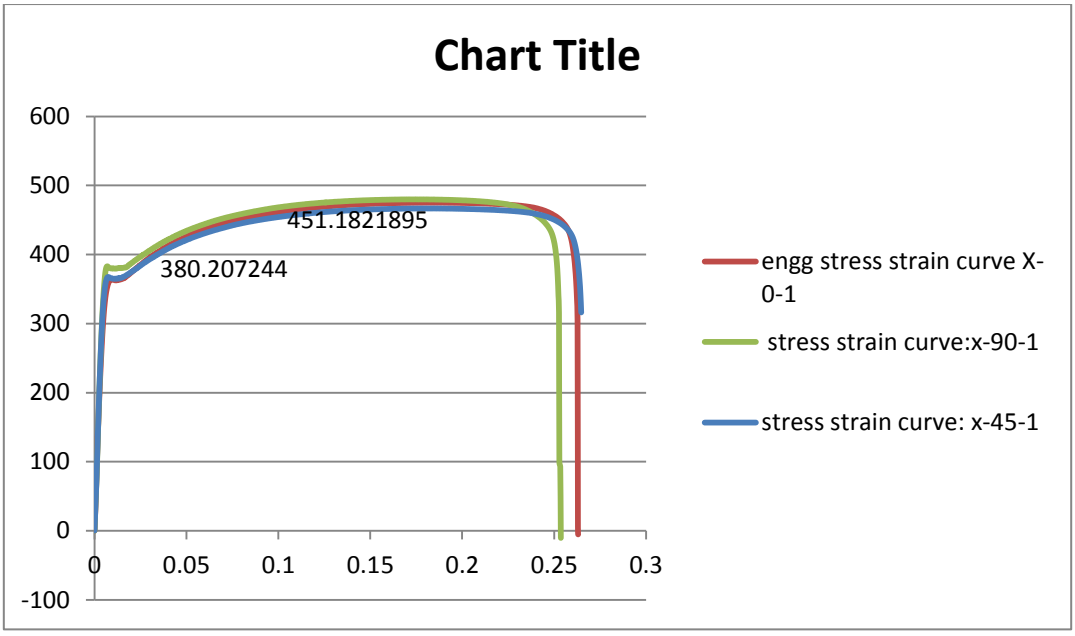

Fig3.5. stress strain curve for sheet thickness 0.9mm.

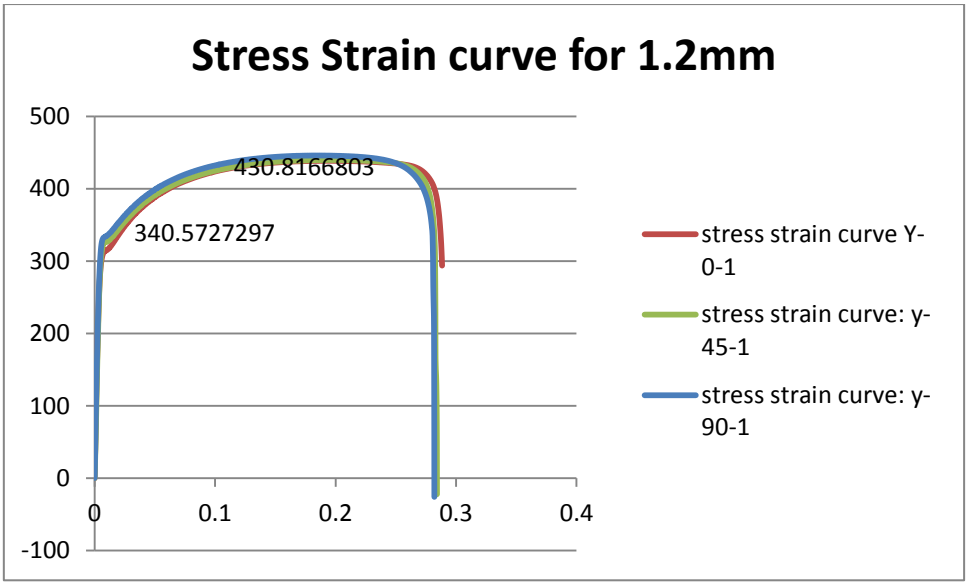

Figure 3.6: stress strain curve for specimen of sheet thickness 1.2mm

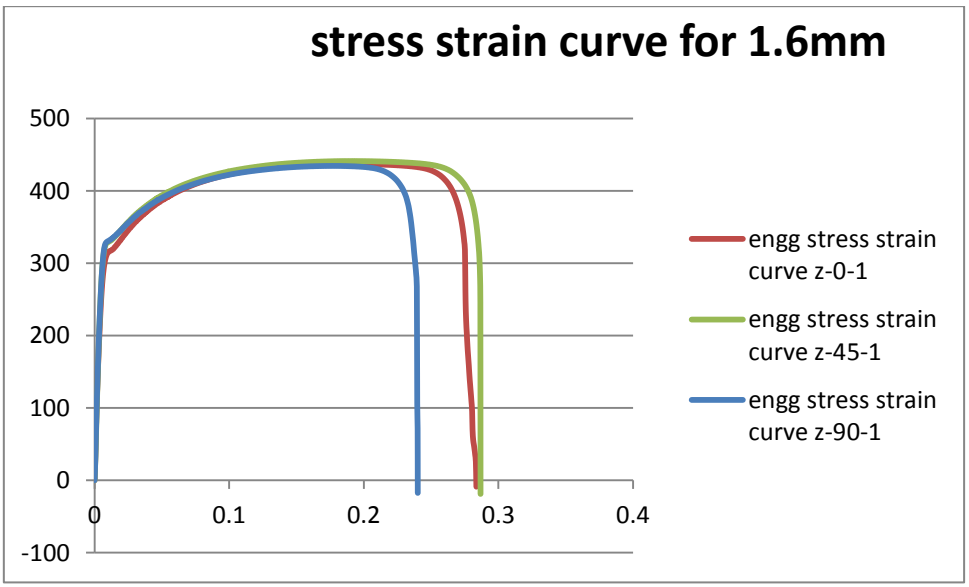

Fig 3.7. : stress strain curve for specimen of sheet thickness 1.6mm

3.3.2 Ductility: The % elongation or the reduction in cross section area is used as a measure of ductility of material. % elongation values were calculated at the fracture. The elongation was measured by fitting together the fractured specimen.

3.3.3 Calculation of Strain hardening exponent (n) and Strength coefficient (K)

The strain hardening exponent (n) and the strength coefficient (K) values are calculated from the stress strain data in uniform elongation region of the stress strain curve. The plot of log (True stress) versus log (True strain) which is a straight line is plotted as discussed below:

The power law of strain hardening is given as

$\sigma = K.\ \varepsilon^{n}$

Where, σ and ε are the true stress and true strain.

Taking log on both sides,

log (σ) = log (K) + n. log (ε)

This is an equation of straight line the slope of which gives the value of ‚n' and K can be calculated taking inverse log of the y-intercept of the line (i.e. log (K)) as shown in Figure 3.9.

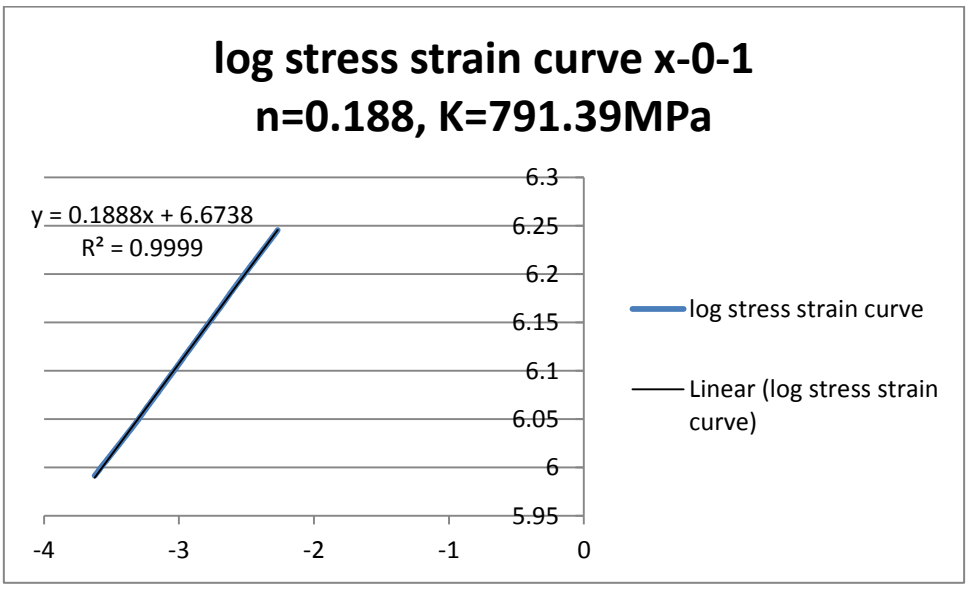

Figure 3.8: Log (True stress) vs. Log (True strain)

3.3.4 Calculation of Anisotropic Parameters:

The R-values at the angles of 0^o, 45^o and 90^o to the rolling direction in the sheet plane were experimentally determined from the tension test.

Procedural Steps:

1. The gauge length of 50 mm was divided into equal intervals of 10 mm each and in each interval the width of the specimen was measured.
2. The tension test was stopped at a predetermined strain value (25% in the present case).
3. The width after elongation of the specimen was measured and using these values the anisotropic parameter was calculated.

The anisotropic parameter 'R' is given by,

$$R = \frac{\varepsilon_w}{\varepsilon_t}$$

Where, εw is the strain in width and εt is the strain in thickness. Since εt is very small value the strain in length is measured as εl.

εw = log(wf / wo)

εl = log(Lf / Lo)

Where, wo and wf are the initial and final width while Lo and Lf are the initial and final length of the specimen.

For constancy of volume, εt= - (εw+ εl)

$$\therefore R = \frac{\varepsilon_w}{-(\varepsilon_l + \varepsilon_w)} = \frac{\log(w_f / w_o)}{\log((w_o * GL_o)/(w_f * GL_f))}$$

Normal anisotropy parameter, $\overline{R}$ is calculated as,

$$\overline{R} = \frac{(R_o + 2R_{45} + R_{90})}{4}$$

3.4 EXPERIMENTAL MEASUREMENT OF SPRINGBACK

3.4.1 Experimental Setup

The experimental setup consists of punch, die, base plate, attachment rod and the blank holder mounted on the double action 100 ton hydraulic press in sheet metal shop. Two sets of punch and die with radius 7.5 mm and 10.0 mm were used for the bending experiments. The punch is attached to the cross-head grip of the UTM through the attachment shank as shown in Figure 3.10. The die was fixed on the base plate on the platform of the press so that any movement of the die can be arrested during bending of the sheets.

The blank holder is required for clamping one of the ends of the sheet during bending.

Fig3.9: INSTRON UNIVERSAL TESTING MACHINE

3.4.2 Fabrication of Tools

As discussed earlier two sets of dies and punches of radius, 7.5 mm and 10 mm were required for the experimental setup of V-bending in addition to other accessories. The included angle for dies and punches was kept as 90degree.

The D-2 tool steel for cold working was selected for the bending dies. The drawings of tooling were made in CATIA-V5 as shown in the figure: 3.10 to 3.17 DXF file was used in EDM-wire cut to fabricate the dies and punches. A total of six dies were designed and two punches with two different punch corner radius. The clearance between dies and punch was made equal to sheet thickness to avoid the localized compressive stresses during bending operation.

The dies and punches were designed with a holding shank of 25mm length and 12.5mm thickness for easy holding and proper alignment in UTM. The setup was designed for UTM for capturing the data for load and deflection.

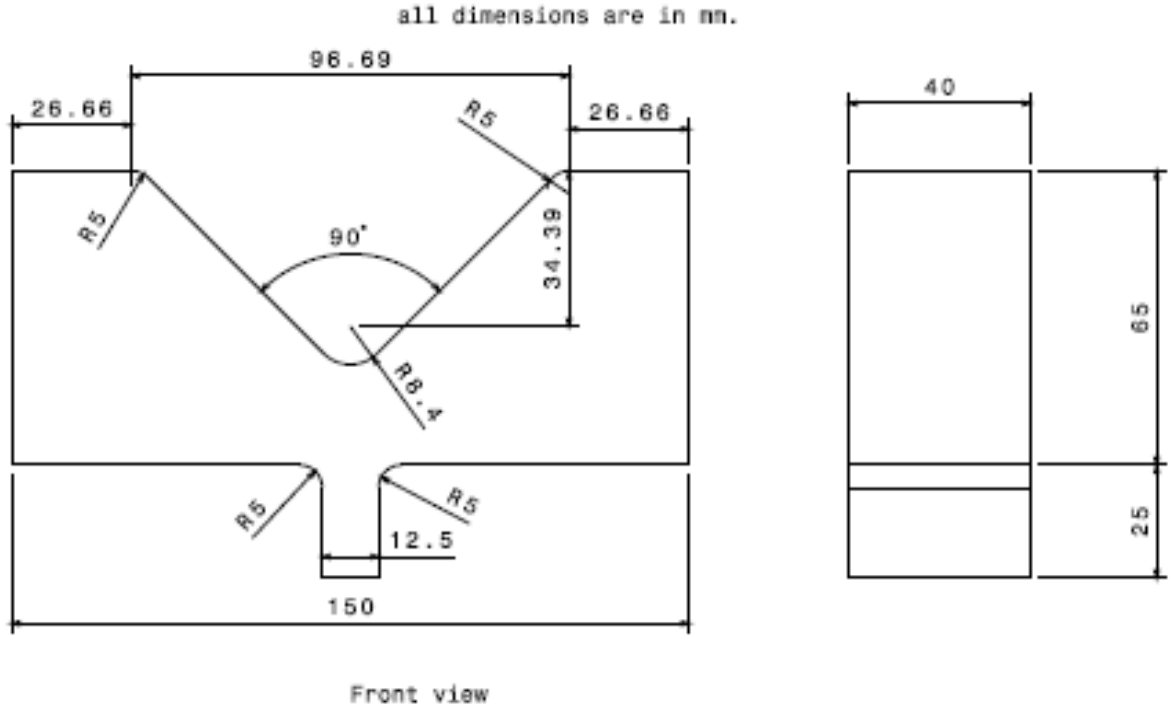

Fig.3.10 Die with corner radii 8.4mm for 0.9mm sheet thickness.

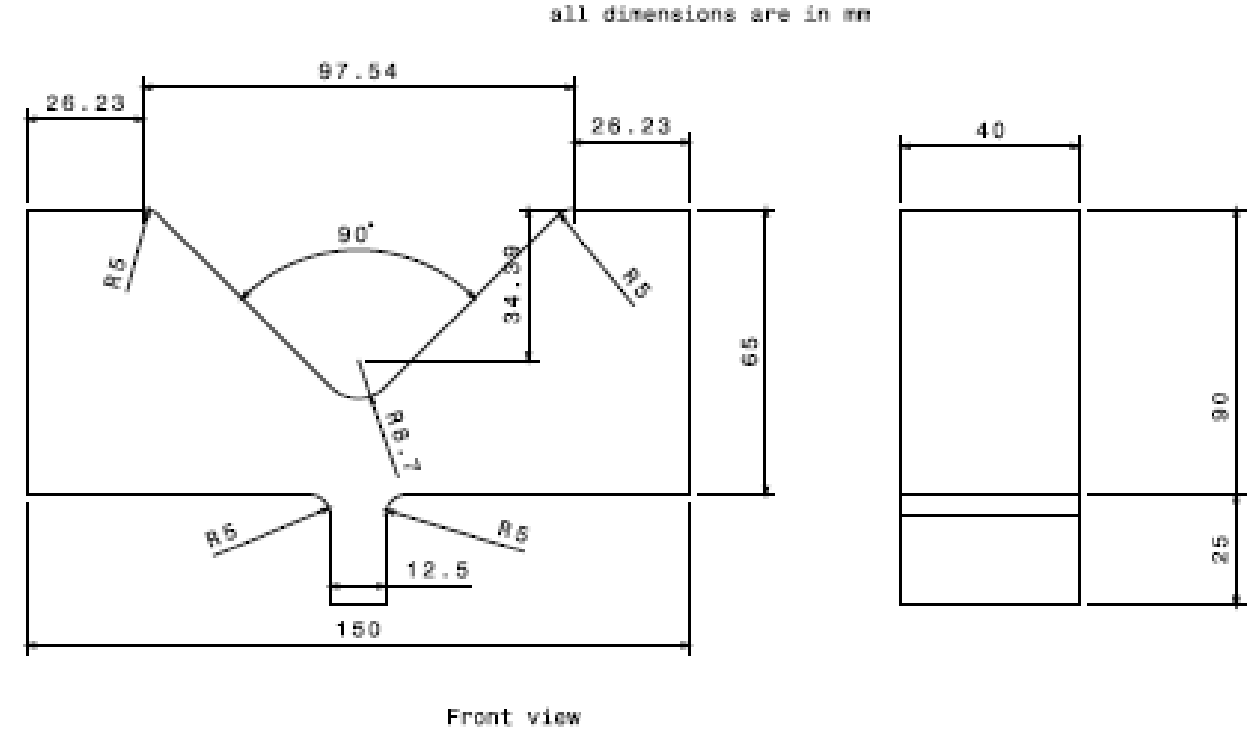

Fig.3.11 Die with corner radii 8.7mm for sheet thickness 1.2mm.

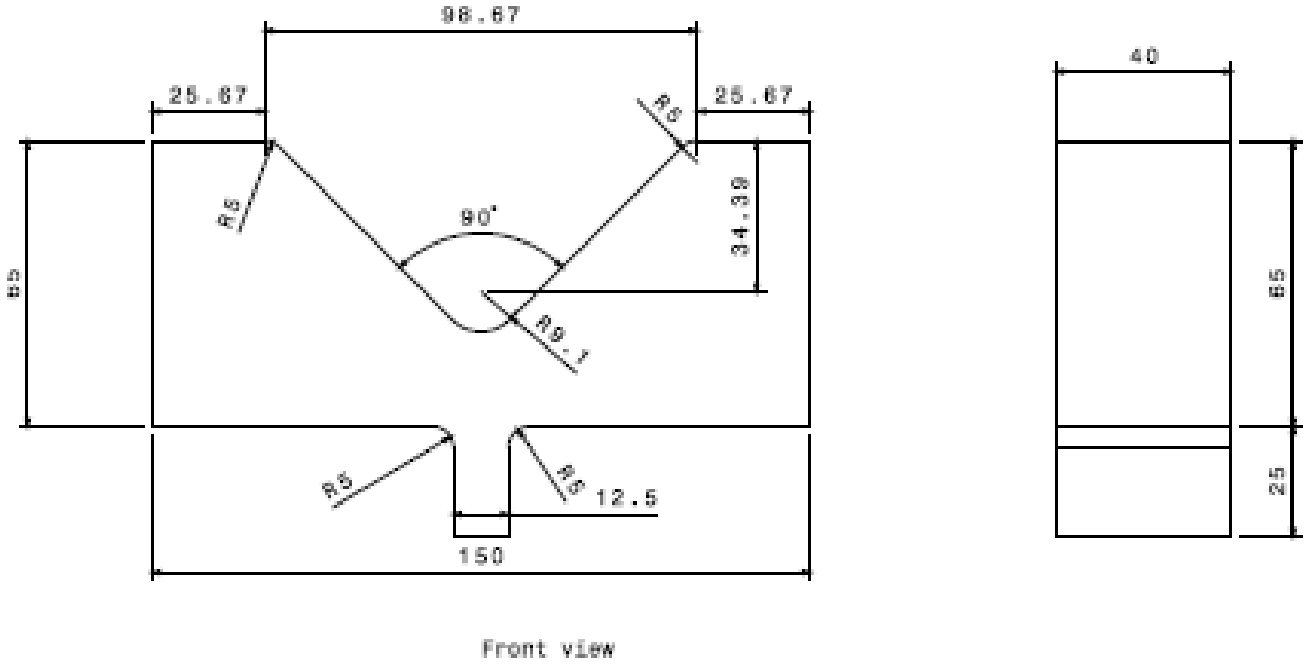

Fig 3.12 Die with corner radii 9.1mm for sheet thickness 1.6mm.

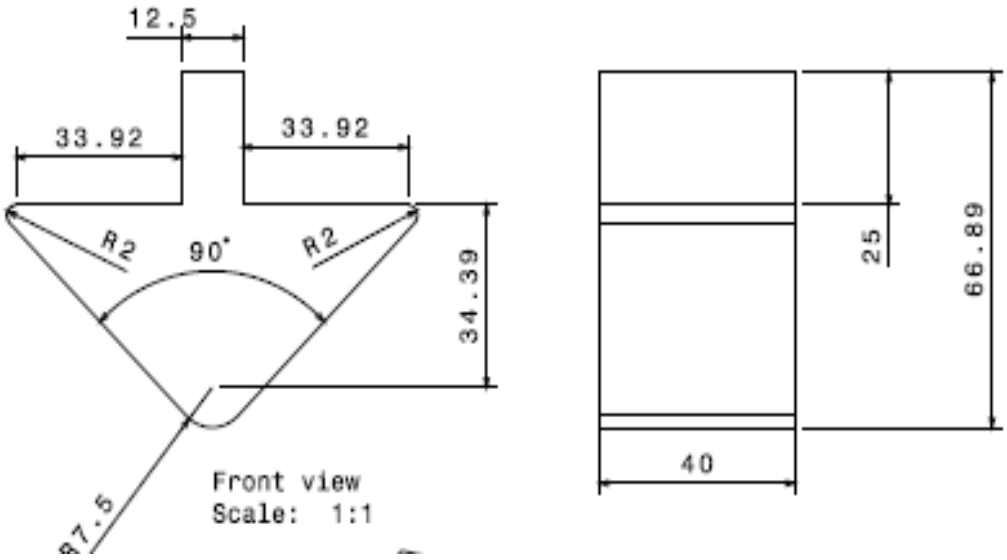

Fig.3.13 Punch with corner radii 7.5mm.

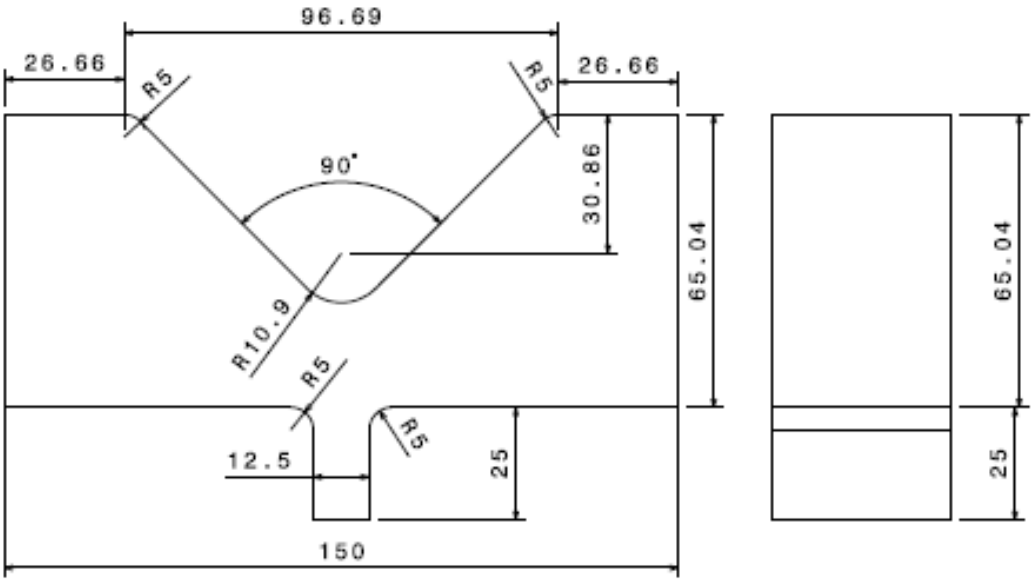

Fig.3.14 Die with corner radius 10.9mm for sheet thickness 0.9mm.

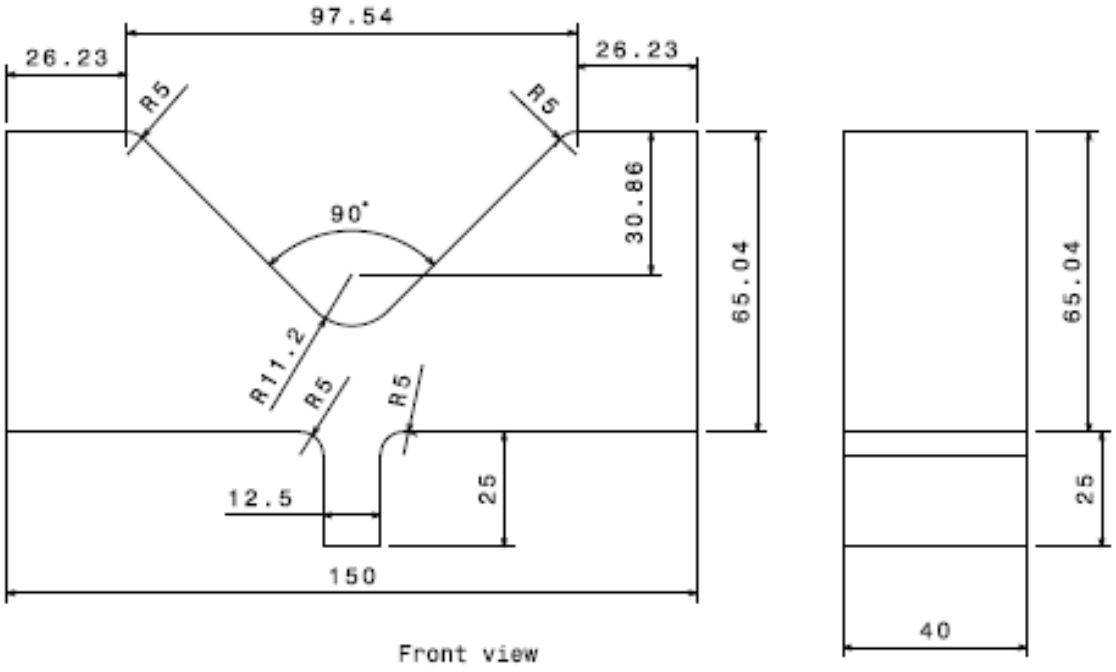

Fig 3.15. Die with corner radii 11.2mm for sheet thickness 1.2mm.

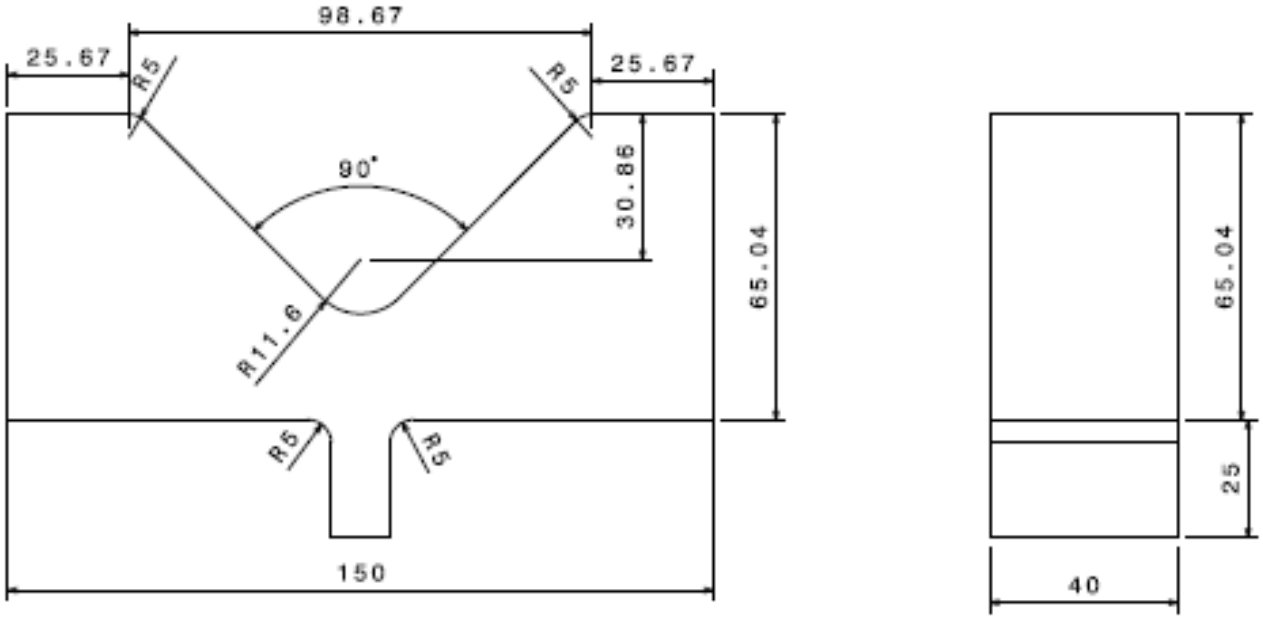

Fig.3.16 Die with corner radii 11.6mm for sheet thickness 1.6mm.

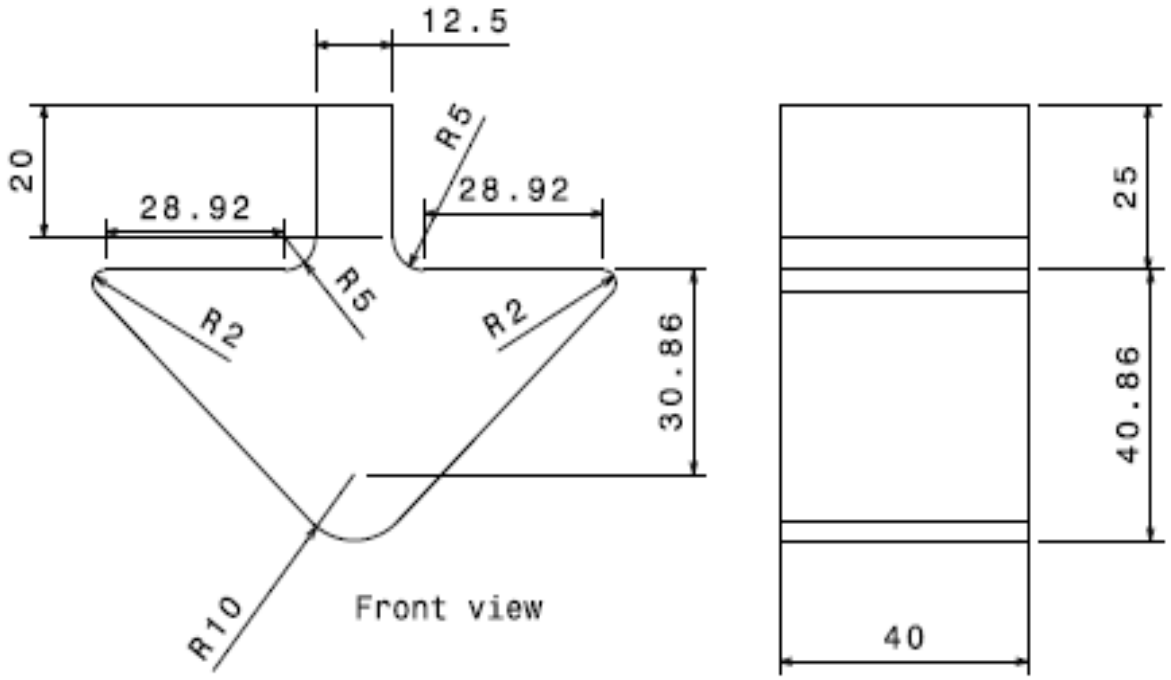

Fig. 3.17 Punch with corner radii 10mm.

3.4.3Heat treatment

D2 steel is preferred for cold working dies. *AISI D2* is a high-carbon(1.6%), high-chromium(12%) tool steel alloyed with molybdenum(1%) and vanadium(1%) characterized by: high wear resistance, high compressive strength, good through-hardening properties, high stability in hardening, and good resistance to tempering-back.

After fabrication the dies and punches were hardened and tempered in Metallurgy laboratory. D-2 steel dies and punches were heated to 910°C in a muffle furnace for 4hrs. And hardened in air and then tempered at 250°C. After air hardening the hardness was 65Rc and after tempering the hardness was 62Rc.

CHAPTER 4

CODE DEVELOPMENT AND THEIR VALIDATION

An analytical model has been developed for the prediction of spring-back perpendicular to the bending axis by modifying the analytical procedure proposed by Raju (2002) for spring-back prediction in conventional sheet materials (parent materials without any change in thickness / properties). The following assumptions have been made:

1. Plain strain condition exists since the w>>t; where w is width of specimen and t is thickness.

2. Neutral axis shift and Bauschinger effect is neglected

To make more accurate prediction of the spring-back by the model the elastic strains during plastic deformation have been considered i.e. elastic plastic material has been considered. The effect of strain hardening is considered according to the power law of hardening. Since the sheets used in the present study are highly anisotropic in the yielding behavior the anisotropy of material has been taken into account by incorporating the anisotropic parameters R0, R45 and R90 in the model.

Let us assume that the specimen is taken such that the width is perpendicular to the rolling direction.

4.1 FINITE ELEMENT METHODS IN SHEET METAL FORMING

There are various engineering methods developed for the deformation analysis of sheet metals in a variety of forming processes. Among these methods, the slip-line field method, the slab method, upper and lower bound techniques are commonly known techniques, and they have been used in calculation of forming loads, shape changes of the deformed blank and in predicting the optimal process conditions. However, an accurate analysis of the effects of process and material parameters on deformation response has become possible when the numerical methods, such as finite difference or finite elements, have developed for these processes. Compared to other numerical approximation techniques, the finite element method is presently the most frequently employed mathematical tool in the computer-aided analysis of sheet metal forming processes.

In method, a set of algebraic equations are derived from the space and time discretized form of virtual work expression using the concept of finite elements [Belytschko et al (2000)].

These finite element equations are solved in order to determine displacements at the element nodal points, which are in-turn input to the clement operator matrices to compute stress and strain tensors at element integration points. When a typical sheet metal forming process is modeled with the FE method, the developed finite element equations possess strong nonlinearities because of the large deformations of the sheet metal, finite strains, changing boundary conditions due to the frictional interface between tooling-sheet metal. Consequently, irrespective of the individual features of the process under consideration, these finite element equations must be solved numerically using incremental procedures based on an explicit time-

integration scheme or incremental-iterative procedures based on an implicit time-integration scheme. Due to this very nature of the forming processes, the finite element simulations of forming processes consume a significant amount of computer resources in the computation of time-histories of nodal displacements and element stresses and strains.

Spring-back is an important and decisive parameter in obtaining the desired geometry of the part and design of the corresponding tooling. In manufacturing industry, it is still a practical problem to predict the final geometry of the part after spring-back and to design appropriate tooling in order to compensate for spring-back. Conventional approaches, which involve using empirical formulae and several trial-and-error procedures, result in wastage of material, time and efforts. In recent years, finite element analysis (FEA) has been considered as an effective way of simulating bending operations and predicting spring-back. FEA provides numerical trial-and-error procedures, which lead to a less time-consuming and more economical way of designing arid producing dies. In particular, some commercially available FEA programs provide effective and powerful tools and environments to model and simulate various operations. These programs include useful and user-friendly graphical user interfaces, which facilitate pre- and post-processing stages.

FEM SIMULATION FOR V-BENDING OPERATION

In this Study all the simulations were performed using the dynamic –explicit FE code, ABAQUS CAE 6.10-1, DASSAULT SYSTEMS Software.

4.2 PROGRAME FLOWCHART AND PROCEDURES

ABAQUS CAE follows the following hierarchy for Simulation:

1. Part
2. Property
3. Assembly
4. Step
5. Interaction
6. Load
7. Mesh
8. Job
9. Visualization
10. sketch

4.2.1PART MODELLING & ASSEMBLY

The modeling comprised of one case:

1. Modeling for V-Bending. Die, punch and the blank were modeled in 2D using ABAQUS software.

Specifications of Die, Punch and Blank setup

- Punch Corner Radius: 7.5mm, 10mm.
- Thickness of Blank: (.9mm, 1.2mm, 1.6mm)

TABLE 4.1 Part Attributes

PARTS	2D
DIE	ANALYTICAL RIGID
PUNCH	ANALYTICAL RIGID
BLANK	DEFORMABLE

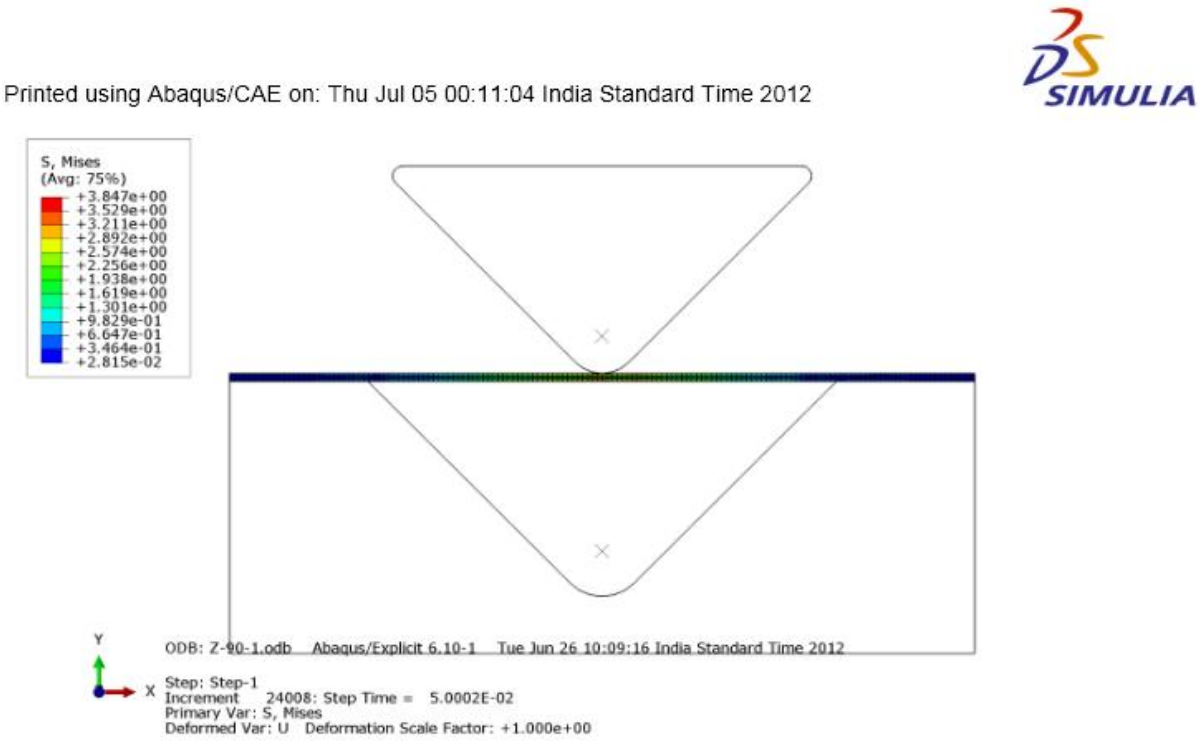

FIGURE 4.1: FEM Setup for 2D Simulation of V-Bending before bending

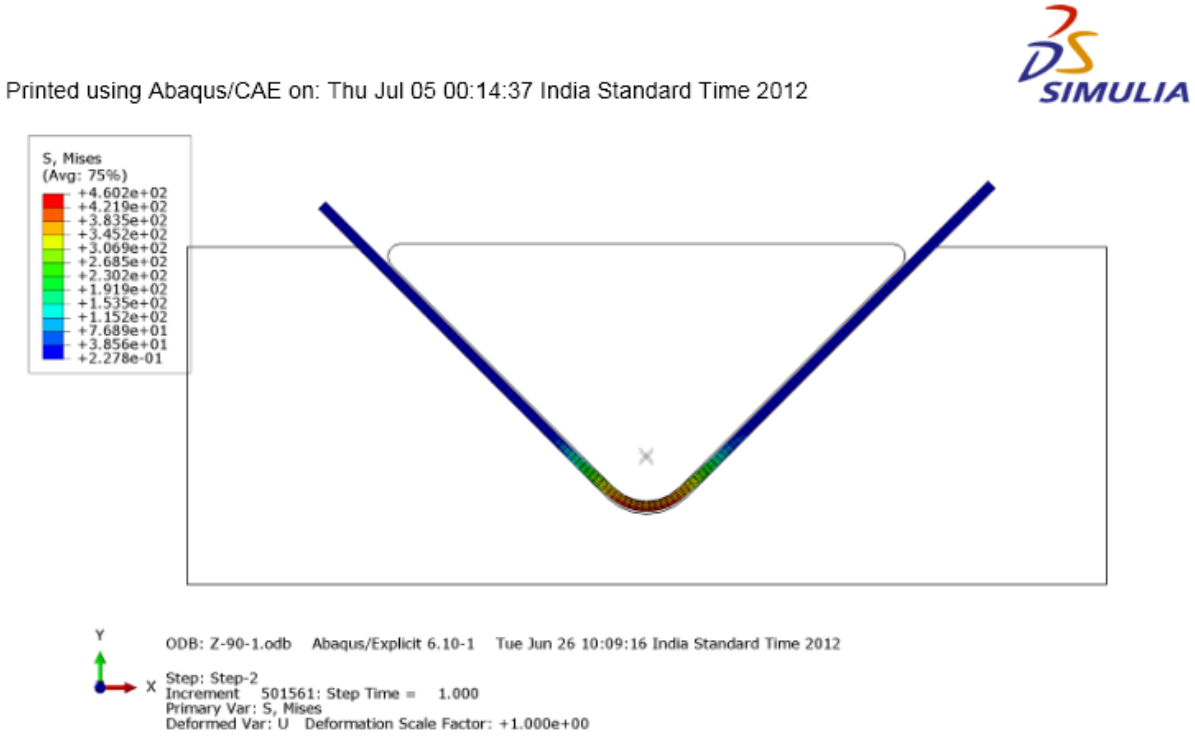

FIGURE 4.2: FEM Setup for 2D Simulation of V-Bending after bending

Improvements in Die

A step was provided in the Die, to prevent shifting at the time of bending and facilitate exact match of the blank surface with that of Die.

4.2.2 MATERIAL PROPERTIES OF BLANK

Properties of IF (Interstitial free) Steel has been imparted to blank:

Mass Density: 7.86E-006 Hardening: Isotropic

Young's Modulus: 210000 Poisson's Ratio: 0.3

Yield Stress	Plastic Strain
350.0682	0
350.3786	0.022314
356.4386	0.024538
356.7644	0.024635
356.9739	0.024731
357.3149	0.024828
357.5255	0.024925
357.72	0.025021
361.1537	0.026373
361.3696	0.026467
361.678	0.026564
361.9962	0.026662
362.2142	0.026758
362.3675	0.026854
362.5808	0.02695
362.929	0.027046
363.106	0.027142
363.3195	0.027238
363.6238	0.027335
363.7787	0.027431
383.3825	0.035965
396.4501	0.042531
420.1642	0.056752
420.8695	0.057219
421.4526	0.057688
422.1979	0.058154

4.2.3 MESH

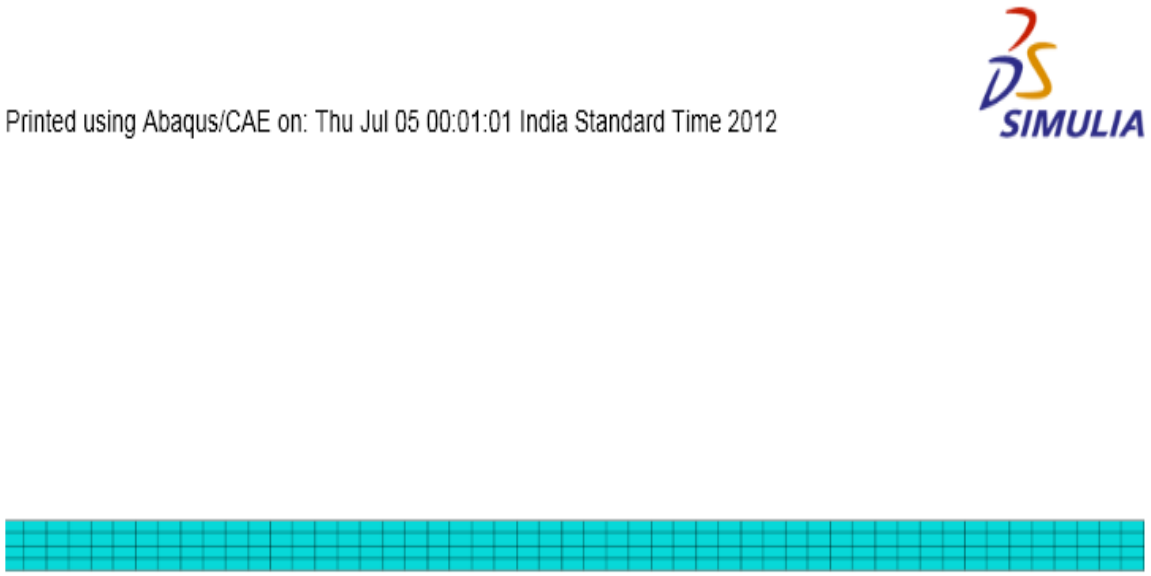

FIGURE 4.3: Meshed Blank

The Parent material model was comprised of:

Total number of nodes: 755

Total number of elements: 600

4.2.4BOUNDARY CONDITIONS

Boundary conditions:

- can be used to specify the values of all basic solution variables (displacements, rotations, warping amplitude, fluid pressures, pore pressures, temperatures, electrical potentials, normalized concentrations, acoustic pressures, or connector material flow) at nodes.
- can be given as “model” input data (within the initial step in Abaqus/CAE) to define zero-valued boundary conditions; and
- can be given as “history” input data (within an analysis step) to add, modify, or remove zero-value or nonzero boundary conditions.
- Boundary conditions specify the Degree of Freedom allowed for a part.

During V-bending Simulation, Die is kept static i.e Degree of Freedom of Die is 0

(a) **DIE** – In Step -1, Boundary Condition imparted to Reference Point of Die is Encastre(i.e dof=0)

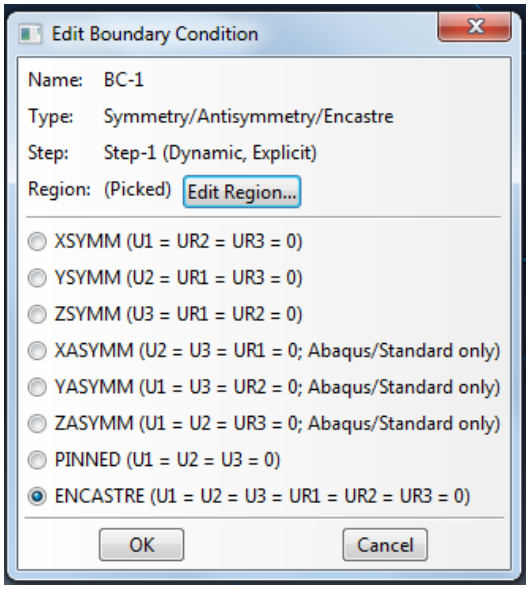

FIGURE 4.4: Boundary Condition for Die.

(b) **PUNCH** -Boundary Condition imparted to Reference Point of Punch is Displacement/Rotation to U2= -0.5 and having rotation = 0radians

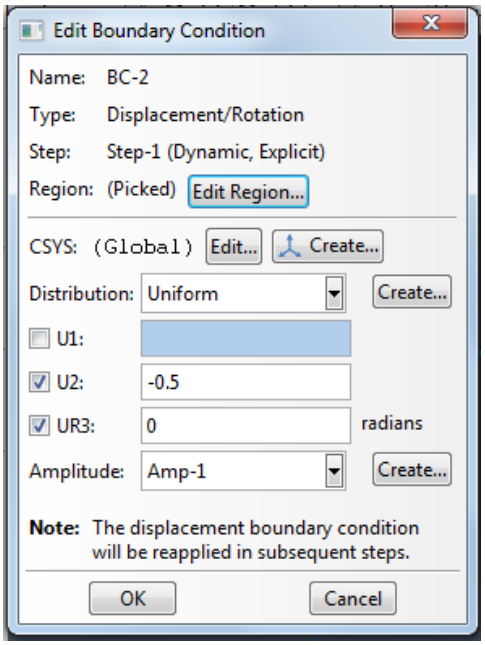

FIGURE 4.5: Boundary Condition for punch

Boundary Condition -3: It specifies the final position of Punch after Displacement from U2= -0.5 to U2=-42.29

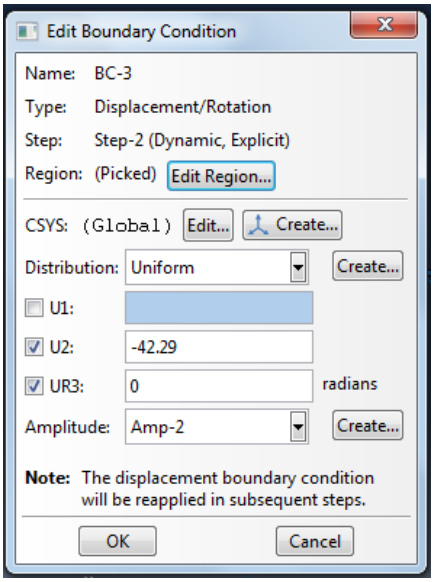

FIGURE 3.6 : Boundary Condition for punch

4.2.5 INTERACTION PROPERTIES

Most contact problems are modeled by using surface-based contact.

Contact between a rigid surface and a deformable body. The structures can be either two or three dimensional, and they can undergo either small or finite sliding. Examples of such problems include metal forming simulations and analyses of rubber seals being compressed between two components.

There are three steps in defining a surface-based contact simulation in Abaqus/Standard:

- defining the surfaces of the bodies that could potentially be in contact;
- specifying which surfaces interact with one another;
- Defining the mechanical and thermal property models that govern the behavior of the surfaces when they are in contact.

In the model two interactions have been specified viz.

Interaction-1 (Friction) & Interaction-2(Frictionless).

Interaction -1: Friction exists between surface of the Die and the bottom surface of BLANK, with coefficient of friction (μ) being 0.1

Interaction-2: There exists no friction between the Punch and top surface of BLANK.

4.2.6 AMPLITUDE

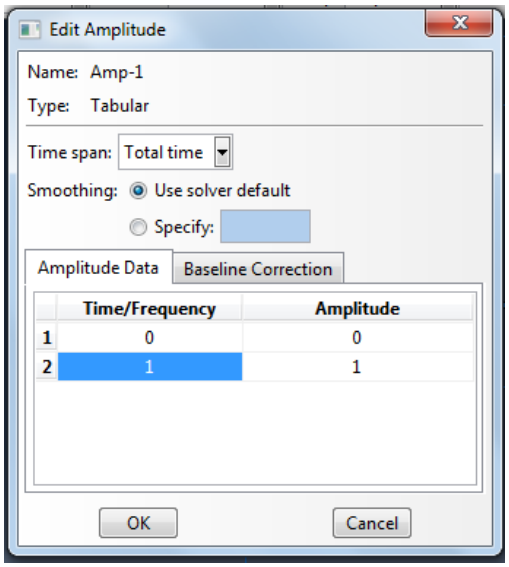

FIGURE 4.7: Amplitude -1 specifying Time/Frequency and Amplitude

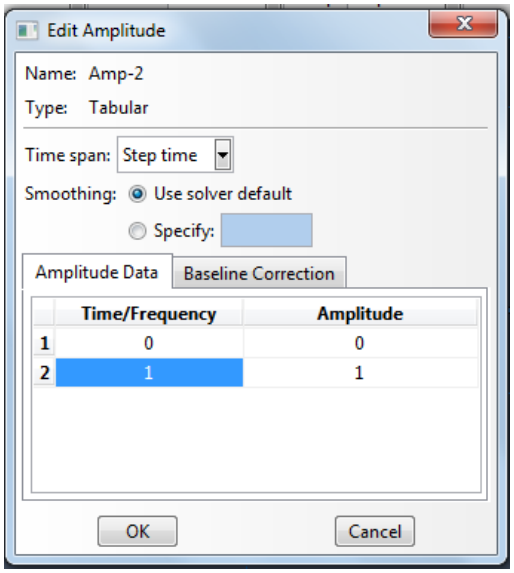

FIUGURE4.8: Amplitude -2 specifying Time/Frequency and Amplitude

4.3 VALIDATION OF CODE AND ITS LIMITATIONS

The Model has been developed using following assumptions:

1. Since thickness to length ratio<<1, therefore the BLANK is assumed to be in Plain strain condition.

2. There exists no friction between Punch and Top surface of blank.

3. The material of Blank is homogeneous.

4. Bauschinger Effect has been neglected.

5. There is no shift of Neutral Axis during V-bending.

CHAPTER 5

RESULTS AND DISCUSSIONS

The results obtained from the analytical and finite element simulation as explained in the previous chapter are presented and discussed below.

5.1 MECHANICAL PROPERTIES

The accuracy of spring-back depends, besides the other factors like mesh size, contact properties, steps given etc., on how accurately the properties of material were tested and supplied as input to simulation. As mentioned earlier, in this study extra low carbon steel of IF (interstitial free) and IFHS (Interstitial free High Strength)grades has been used. This material has very low carbon content (0.001 – 0.003 %) and hence very good formability. The tension tests results for Parent material is tabulated in Table 5.1.

TABLE 5.1: MECHANICAL PROPERTIES OF MATERIAL

MATERIAL	THICKNESS (mm)	YOUNG'S MODULUS (MPA)	ANGLE WITH ROLLING DIRECTION	HARDENING MODULUS (k)	STRAIN HARDENING COEFFICIENT (n)
IFHS	0.9	210000	0˚ 45˚ 90˚	791.39 762 785.4	0.188 0.179 0.1798
IFHS	1.2	210000	0˚ 45˚ 90˚	744.7 730.18 741.7	0.199 0.190 0.188
IFHS	1.6	21000	0˚ 45˚ 90˚	735.9 732 716.51	0.196 0.192 0.184

5.2 SPRINGBACK RESULTS

The FEA Simulation of Spring-back of material:

1. IFHS 0.9mm (Isotropic) with punch corner radii 7.5mm.
2. IFHS 1.2mm (Isotropic) with punch corner radii 7.5mm.
3. IFHS 1.6mm (Isotropic) with punch corner radii 7.5mm.
4. IFHS 0.9mm (Isotropic) with punch corner radii 10mm.
5. IFHS 1.2mm (Isotropic) with punch corner radii 10mm.
6. IFHS 1.6mm (Isotropic) with punch corner radii 10mm.

CASE 1: IFHS 0.9mm (Isotropic) with punch corner radii 7.5mm.

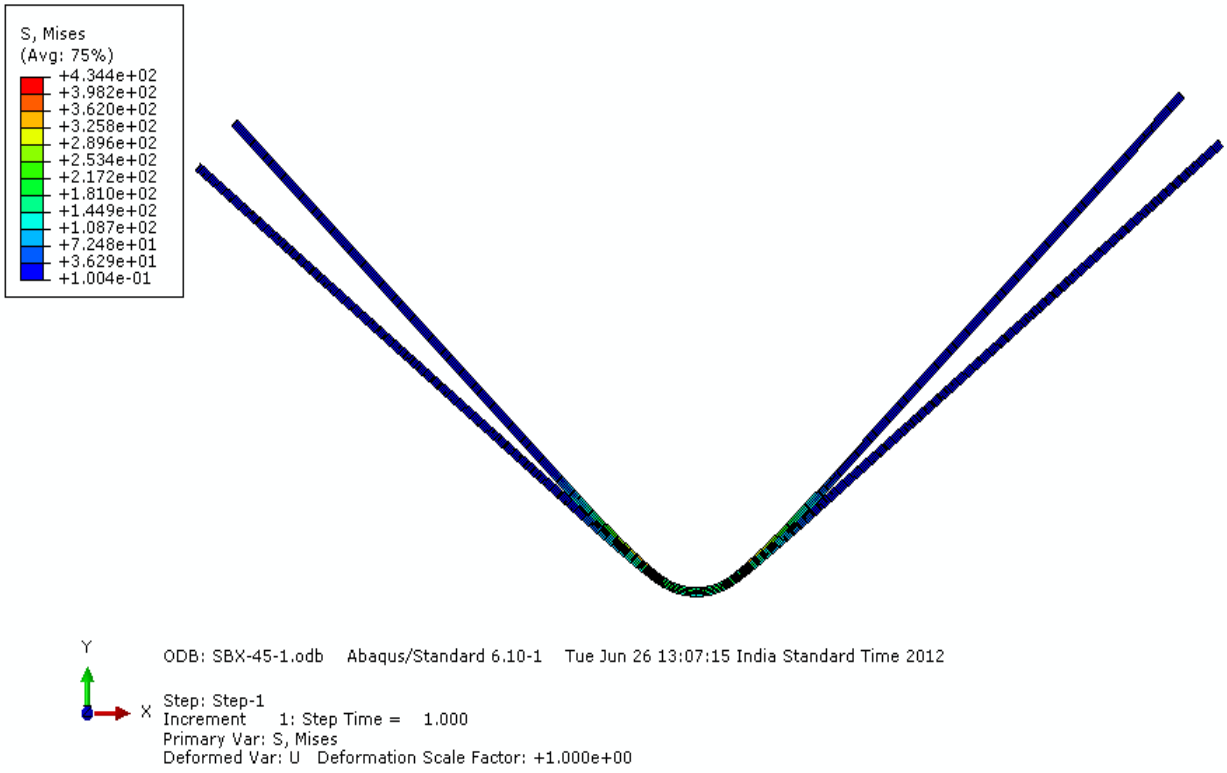

Fig. 4.9 IFHS 0.9mm (Isotropic) with punch corner radii 7.5mm.

Spring-back observed = $\alpha_f - \alpha_i = 4.12^o$

Operator name: PARVEEN KUMAR

Sample Identification: VR84P75Z01

Test Method Number: 0

General Compression Test -US Customary Units

Test Date:	Friday, May 18, 2012
Interface Type:	5500
Crosshead Speed:	15.0000mm/mi
Second Speed:	0.0000mm/min
Third Speed:	0.0000mm/min
Sample Rate (pts/secs):	10.0000
Temperature:	73 F
Humidity (%):	50
Specimen G. L.:	101.6000mm
Extensometer G.L:	50.800mm

	Displacement at Max. Load (mm)	Load at Max. Load (kN)
1	42.979	4.007
Mean	42.979	4.007
S.D	0	0

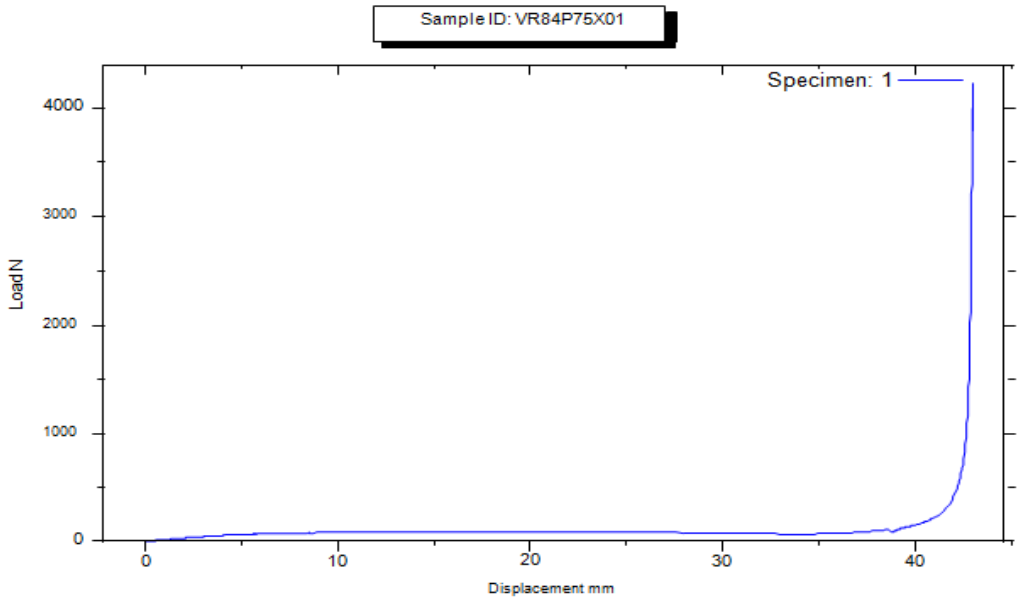

Fig.4.10 load vs. displacement curve for 0.9mm sheet thickness with high load.

Operator name: PARVEEN KUMAR

Sample Identification: VR87P75Y01

Test Method Number: 0

General Compression Test - US Customary Units

Test Date:	Wed, May 16, 2012
Interface Type:	5500
Crosshead Speed:	15.0000
Second Speed:	0.0000
Third Speed:	0.0000
Sample Rate (pts./sec):	10.0000
Temperature:	73 F
Humidity (%):	50
Specimen G. L.:	101.5999
Extensometer G.L.:	50.8000

	Displacement at Max. Load (mm)	Load at Max. Load (kN)
1	43.150	1.220
Mean	43.150	1.220
S.D	0	0

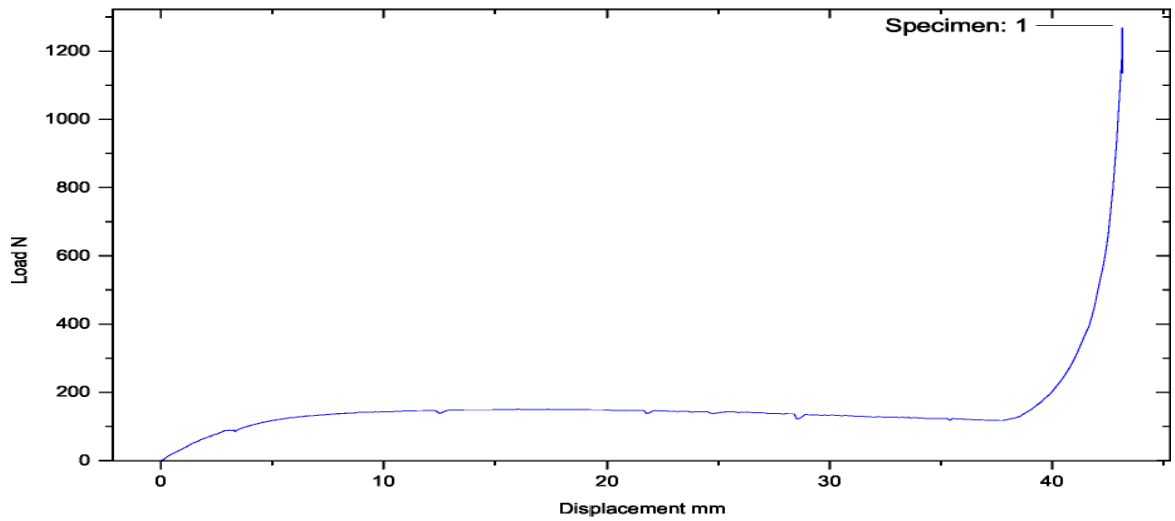

Fig.4.11 load vs. displacement curve for 1.2mm sheet thickness with high load.

Operator name: PARVEEN KUMAR

Sample Identification: VR91P75Z01

Test Method Number: 0

General Compression Test -US Customary Units

Test Date:	Friday, May 18, 2012
Interface Type:	5500
Crosshead Speed:	15.0000mm/min
Second Speed:	0.0000mm/min
Third Speed:	0.0000mm/min
Sample Rate (pts/secs):	10.0000
Temperature:	73 F
Humidity (%):	50
Specimen G. L.:	101.6000mm
Extensometer G.L:	50.800 mm

	Displacement at Max. Load (mm)	Load at Max. Load (kN)
1	42.599	2.500
Mean	42.599	2.500
S.D	0	0

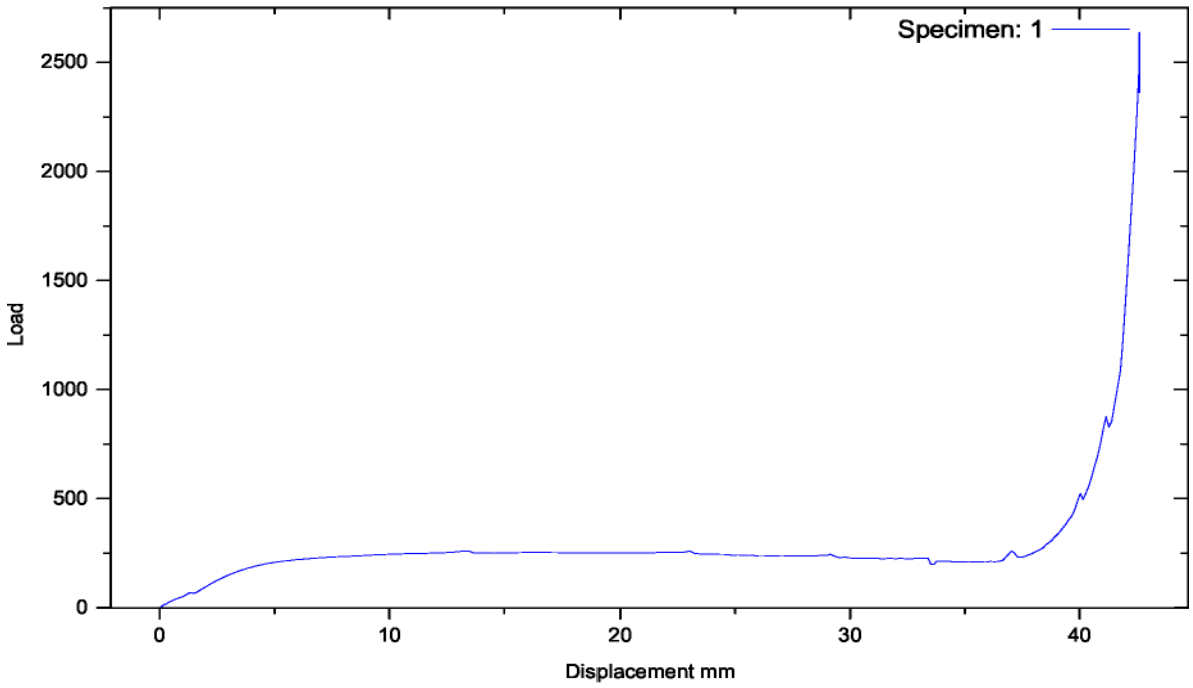

Fig.4.12 load vs. displacement curve for 1.6mm sheet thickness with high load.

CASE 2: IFHS 1.2mm (Isotropic) with punch corner radii 7.5mm.

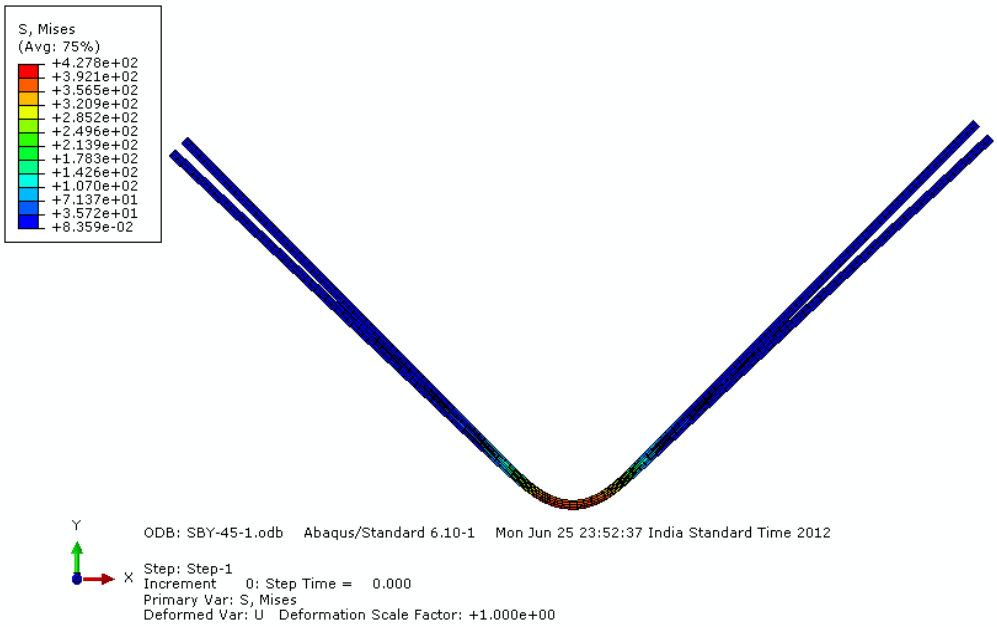

Fig. 4.13: IFHS 1.2mm (Isotropic) with punch corner radii 7.5mm.

Spring-back observed = $\alpha_f - \alpha_i = 2^{\circ}$

CASE 3: IFHS 1.6mm (Isotropic) with punch corner radii 7.5mm.

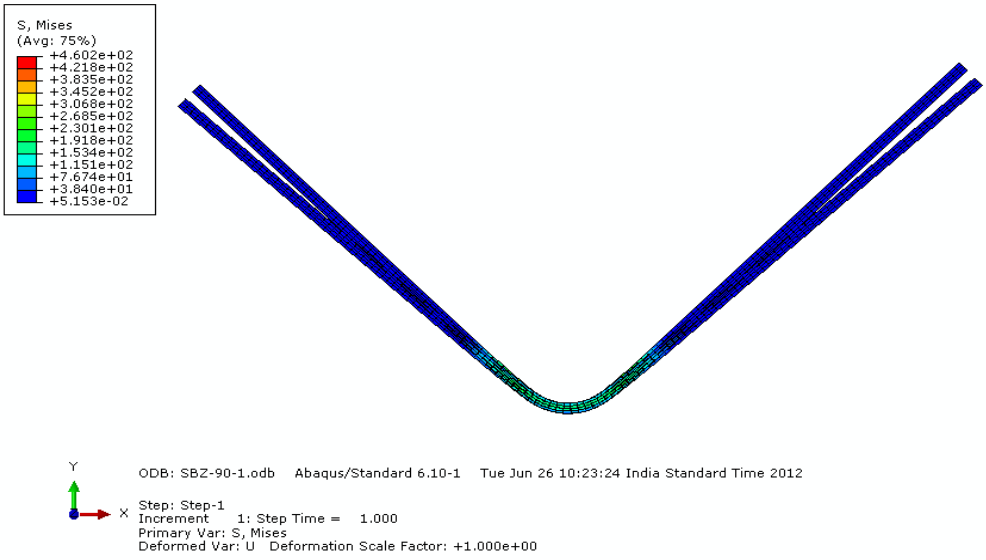

Fig.4.14 IFHS 1.6mm (Isotropic) with punch corner radii 7.5mm.

Spring-back observed = $\alpha_f - \alpha_i = 2.61^{\circ}$

SHEET WITH DIFFERENT THICKNESS (in mm)	ROLLING DIRECTION	Load (kN)	EXPERIMENTAL (IN DEGREE)	ANALYTICAL (IN DEGREE)	BY SIMULATION (IN DEGREE)
0.9	0˚	4.007	3.615˚	2.81˚	4.12˚
0.9	45˚	3.659	4.66˚	3.78˚	5.46˚
0.9	90˚	4.008	4.61˚	3.57˚	5.33˚
1.2	0˚	1.202	.9695˚	.9124˚	1.21˚
1.2	45˚	2.466	1.70˚	1.50˚	2˚
1.2	90˚	1.698	3.24˚	1.65˚	1.1˚
1.6	0˚	2.500	1.52˚	1.56˚	1.42˚
1.6	45˚	2.501	2.38˚	1.90˚	1.73˚
1.6	90˚	2.501	2.32˚	1.95˚	2.62˚

Table5.2. SPRING BACK DUE TO HIGH LOAD WITH PUNCH CORNER RADII 7.5mm.

CASE 4: IFHS 0.9mm (Isotropic) with punch corner radii 10mm.

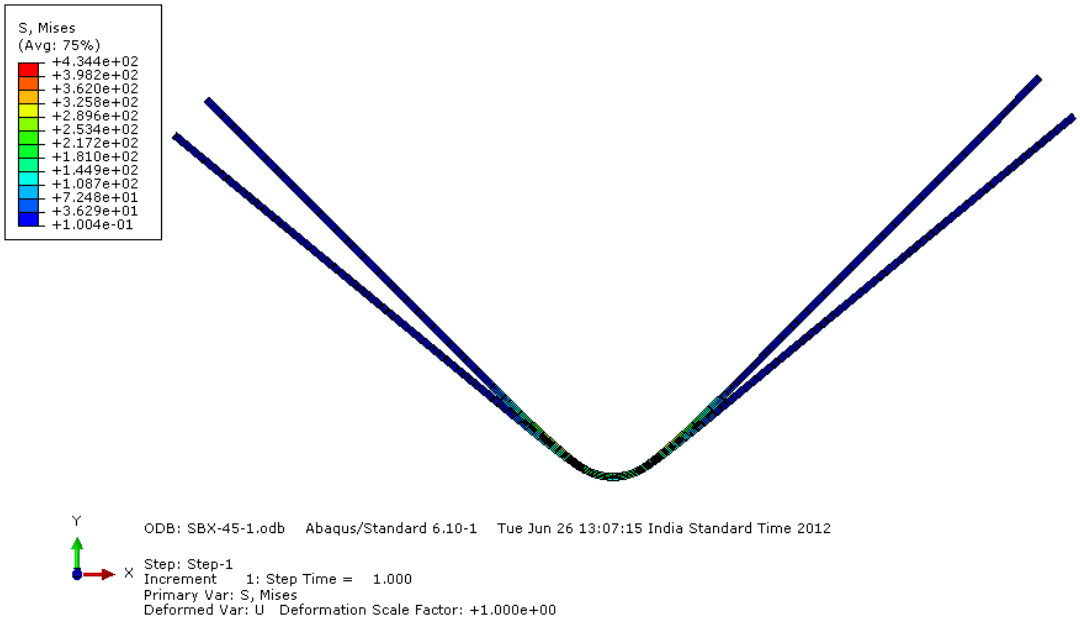

Fig.4.15: IFHS 0.9mm (Isotropic) with punch corner radii 10mm.

Spring-back observed = $\alpha_f - \alpha_i$ = 4.45˚

CASE 5:IFHS 0.9mm (Isotropic) with punch corner radii 10mm.

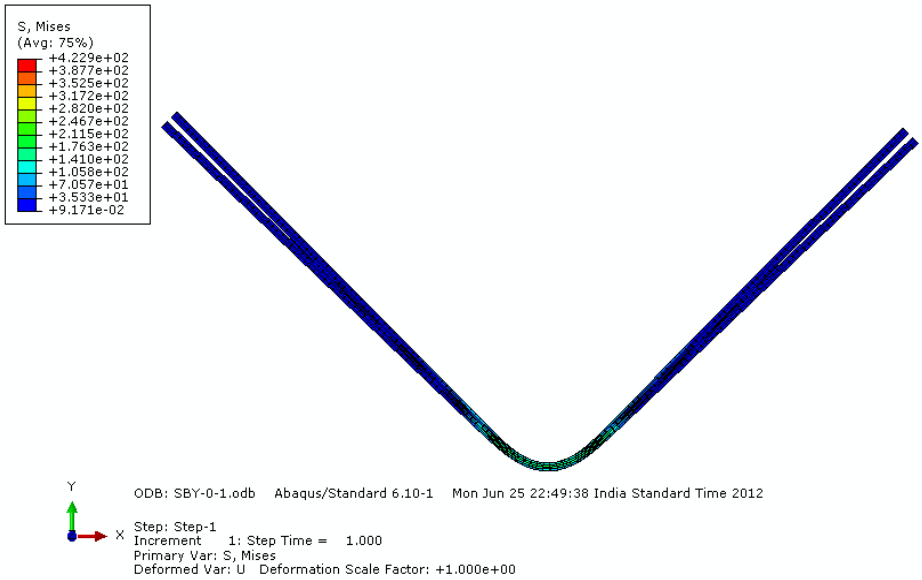

Fig 4.16: IFHS 1.2mm (Isotropic) with punch corner radii 10mm.

Spring-back observed = $\alpha_f - \alpha_i = 2.68^{\circ}$

CASE 6: IFHS 1.6mm (Isotropic) with punch corner radii 10mm.

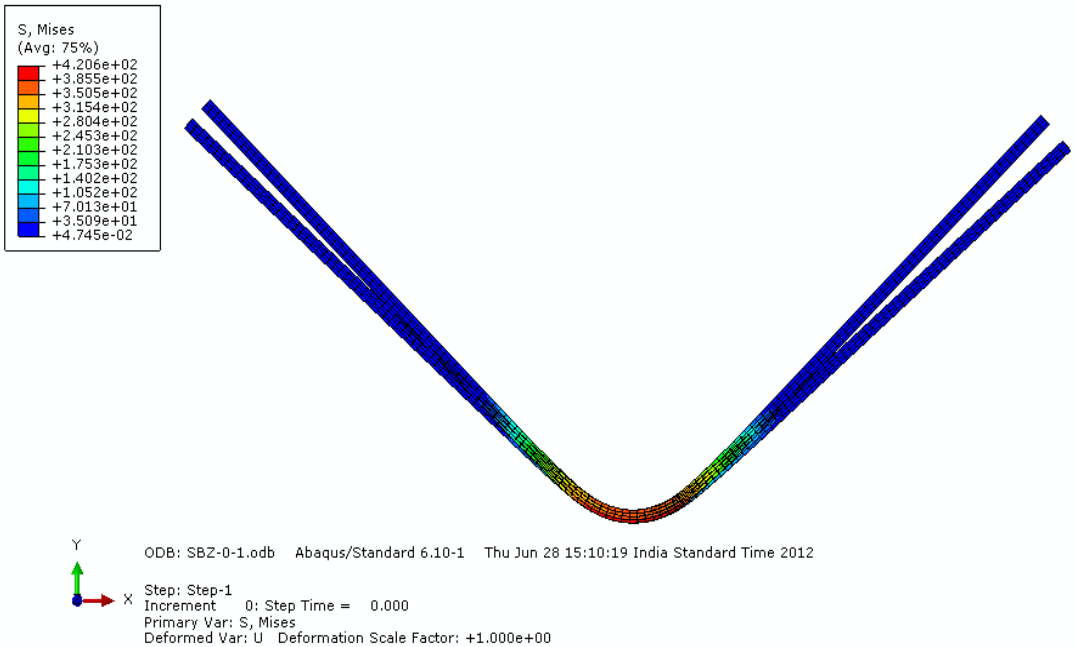

Fig.4.17: IFHS 1.6mm (Isotropic) with punch corner radii 10mm.

Spring-back observed = $\alpha_f - \alpha_i = 3.07^{\circ}$

SHEET WITH DIFFERENT THICKNESS (in mm)	ROLLING DIRECTION	EXPERIMENTAL (IN DEGREE)	ANALYTICAL (IN DEGREE)	BY SIMULATION (IN DEGREE)
0.9	0˚	4.15˚	3.76	4.45˚
0.9	45˚	4.92˚	4.38˚	5.32˚
0.9	90˚	5.11˚	4.74˚	5.44˚
1.2	0˚	2.84˚	2.12˚	2.68˚
1.2	45˚	3.69˚	2.34˚	2.48˚
1.2	90˚	3.81˚	1.93˚	1.79˚
1.6	0˚	2.58˚	2.56˚	2.86˚
1.6	45˚	2.71˚	1.82˚	1.74˚
1.6	90˚	3.08˚	2.78˚	3.07˚

Table 5.3: SPRING BACK DUE TO HIGH LOAD WITH PUNCH CORNER RADII 10mm.

EFFECT OF MESHING ONBALNK SHIFT

The results of any FEA Simulation greatly depend on the type of meshing done. It was observed that when the mesh size was large enough, blank was subjected to greater shift, even though mesh was Quad dominated and free from distorted elements. However when the meshing was changed incorporating a finer element size, there was an significant reduction in blank shift.

5.3 Stress Distribution during bending

During the bending process, the existence of an elastic core could be easily identified as the central region with the minimum stresses. This elastic core is responsible for the Spring-back of the blank.

The region of BLANK in contact with the punch has maximum stresses induced in it.

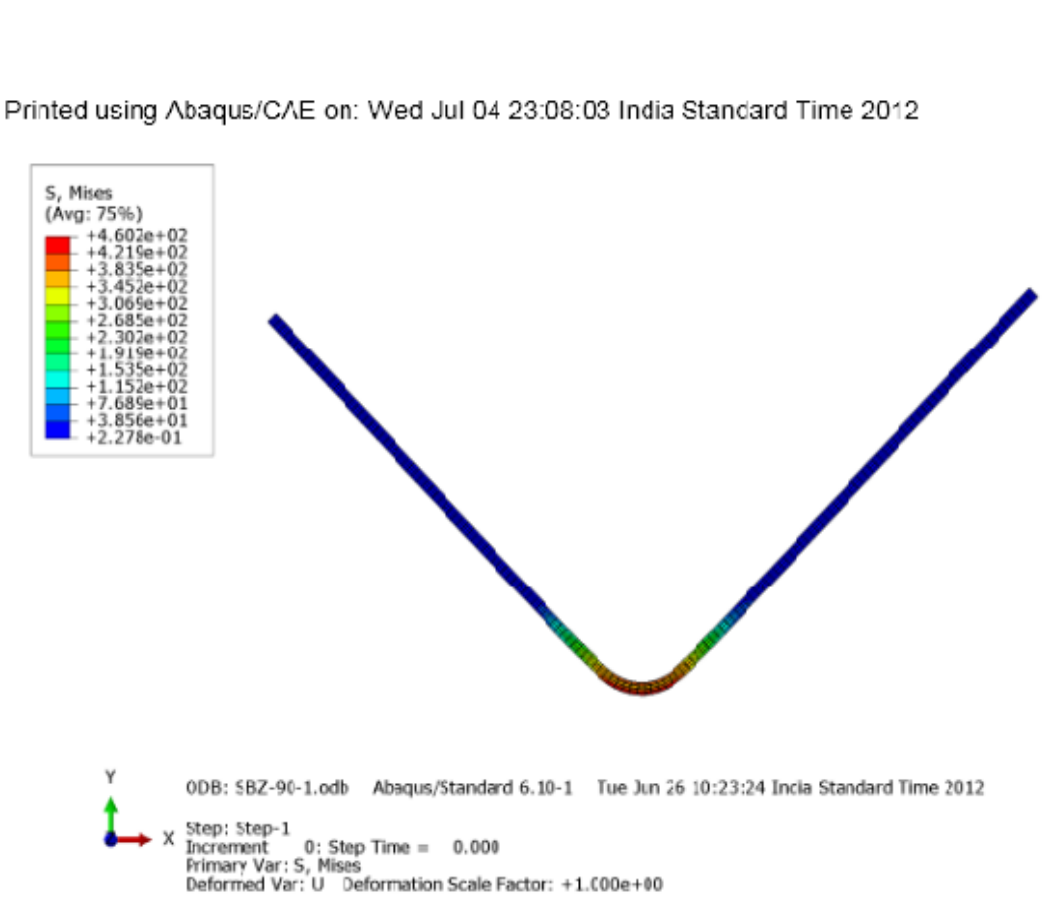

Fig 4.18 Stress distribution during bending.

SHEET WITH DIFFERENT THICKNESS (in mm)	ROLLING DIRECTION	Load in (kN)	EXPERIMENTAL (IN DEGREE)	ANALYTICAL (IN DEGREE)	BY SIMULATION (IN DEGREE)
0.9	0˚	.300	4.615˚	5.41˚	4.12˚
0.9	45˚	.300	5.66˚	5.88˚	5.46˚
0.9	90˚	.300	4.81˚	5.57˚	5.33˚
1.2	0˚	.800	1.21˚	1.91˚	1.41˚
1.2	45˚	.800	1.90˚	2.50˚	2.21˚
1.2	90˚	.400	3.44˚	3.65˚	3.10˚
1.6	0˚	1.00	1.92˚	2.16˚	1.62˚
1.6	45˚	0.313	2.78˚	2.90˚	2.13˚
1.6	90˚	1.00	3.12˚	3.35˚	2.92˚

Table 5.4: SPRING BACK DUE TO LOW LOAD WITH PUNCH CORNER RADII 7.5mm.

Operator name: PARVEEN KUMAR

Sample Identification: VR84P75X01

Test Method Number: 0

General Compression Test -US Customary Units

Test Date:	Friday, May 18, 2012
Interface Type:	5500
Crosshead Speed:	15.0000mm/min
Second Speed:	0.0000mm/min
Third Speed:	0.0000mm/min
Sample Rate (pts/secs):	10.0000
Temperature:	73 F
Humidity (%):	50
Specimen G. L.:	101.6000mm
Extensometer G.L:	50.800 mm

	Displacement at Max. Load (mm)	Load at Max. Load (kN)
1	41.179	0.300
Mean	41.179	0.300
S.D	0	0

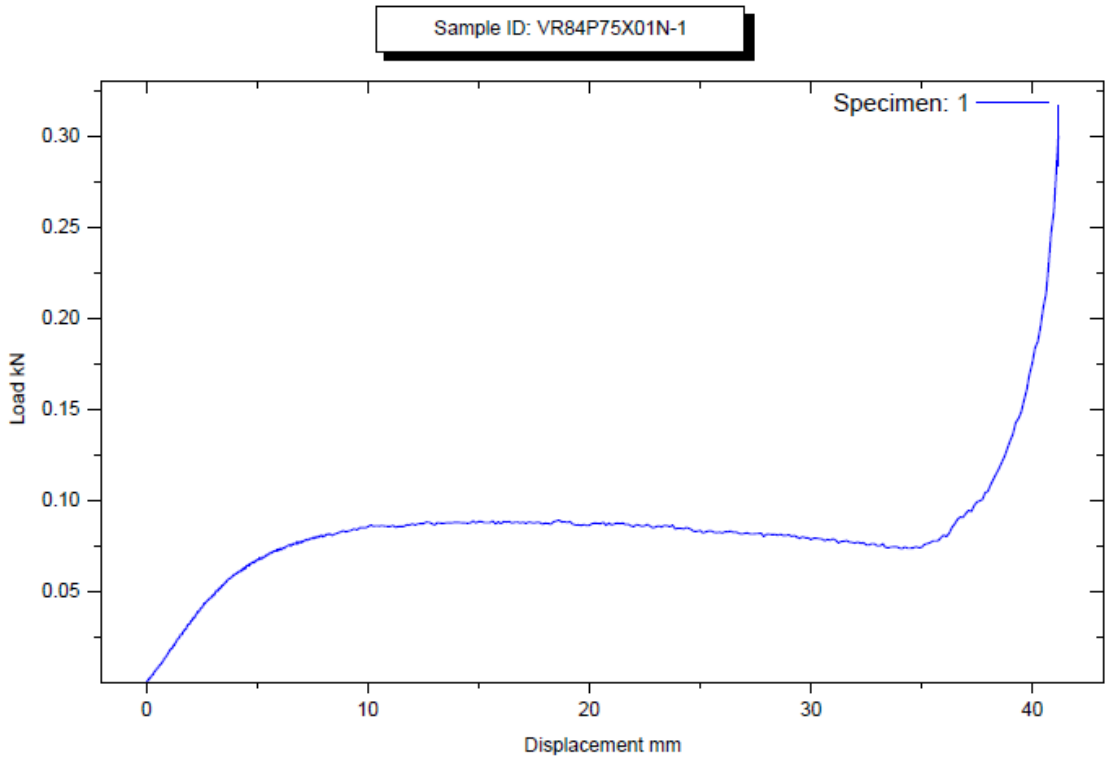

Fig.4.19: load vs. displacement curve for 0.9mm sheet thickness with low load.

Operator name: PARVEEN KUMAR

Sample Identification: VR87P75Y01

Test Method Number: 0

General Compression Test -US Customary Units

Test Date:	Friday, June 08, 2012
Interface Type:	5500
Crosshead Speed:	15.0000mm/min
Second Speed:	0.0000mm/min
Third Speed:	0.0000mm/min
Sample Rate (pts/secs):	10.0000
Temperature:	73 F
Humidity (%):	50
Specimen G. L.:	101.6000mm
Extensometer G.L:	50.800 mm

	Displacement at Max. Load (mm)	Load at Max. Load (kN)
1	42.505	0.800
Mean	42.505	0.800
S.D	0	0

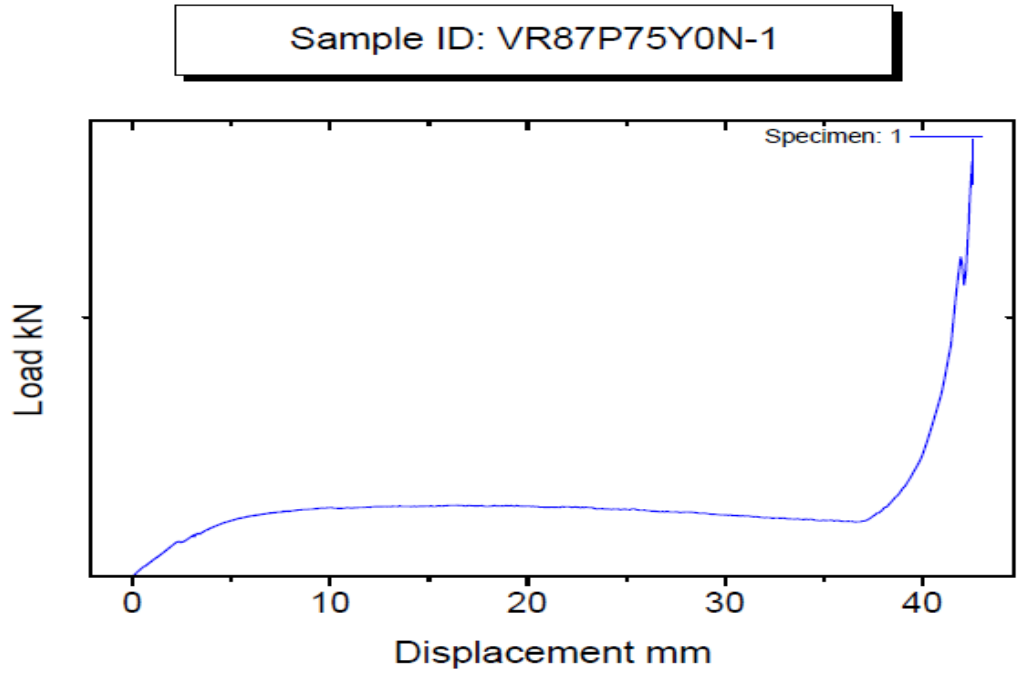

Fig.4.20: load vs. displacement curve for 1.2mm sheet thickness with low load.

Operator name: PARVEEN KUMAR

Sample Identification: VR91P75Z01

Test Method Number: 0

General Compression Test -US Customary Units

Test Date:	Friday, June 08, 2012
Interface Type:	5500
Crosshead Speed:	15.0000mm/min
Second Speed:	0.0000mm/min
Third Speed:	0.0000mm/min
Sample Rate (pts/secs):	10.0000
Temperature:	73 F
Humidity (%):	50
Specimen G. L.:	101.6000mm
Extensometer G.L:	50.800 mm

	Displacement at Max. Load (mm)	Load at Max. Load (kN)
1	41.832	1.00
Mean	41.832	1.00
S.D	0	0

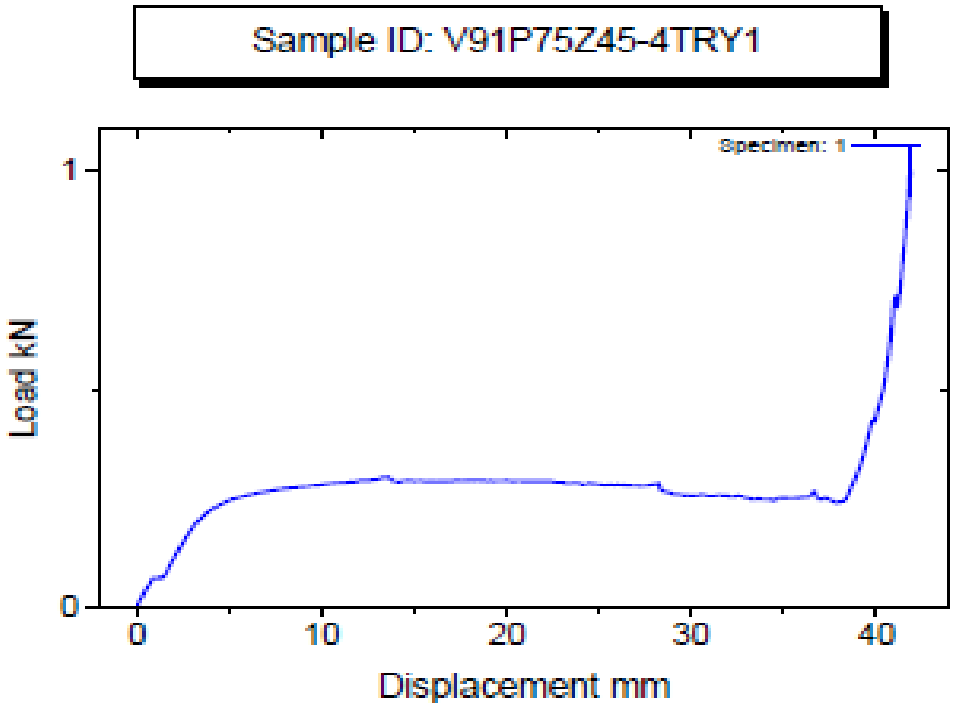

Fig.4.21: load vs. displacement curve for 1.6mm sheet thickness with low load.

SHEET WITH DIFFERENT THICKNESS (in mm)	ROLLING DIRECTION	EXPERIMENTAL (IN DEGREE)	ANALYTICAL (IN DEGREE)	BY SIMULATION (IN DEGREE)
0.9	0˚	5.15˚	5.76	5.45˚
0.9	45˚	5.92˚	5.98˚	5.82˚
0.9	90˚	5.11˚	5.74˚	5.54˚
1.2	0˚	3.14˚	3.52˚	3.48˚
1.2	45˚	3.49˚	3.74˚	3.18˚
1.2	90˚	3.91˚	4.13˚	3.79˚
1.6	0˚	2.18˚	2.96˚	2.56˚
1.6	45˚	1.94˚	2.12˚	1.94˚
1.6	90˚	2.98˚	3.18˚	3.07˚

Table 5.5: SPRING BACK DUE TO LOW LOAD WITH PUNCH CORNER RADII 10mm.

CHAPTER 6

6.1CONCLUSIONS

1. Spring-back on the basis of anisotropy: the strength of the sheet was found to be more in 90˚ to the rolling direction and the spring back was found to be more analytically and experimentally.
2. Effect of thickness on spring-back, as the thickness of material increases the spring-back decreases.
3. Effect of punch corner radii, as the punch corner radii increases the spring-back effect increases.
4. Experiments show that the spring-back can be effectively compensated by localization (shown in table 5.2) of compressive stresses by the increase in the load in the final phase of bending when the sheet is conforming to the shape of the die fully.

6.2 SCOPE FOR FUTURE WORK

1. An FEA program can be written for spring-back compensation by localized compressive force on the basis of sheet-metal strength and sheet thickness.
2. Straining the sheet while bending can effectively reduce compensation and studies can be carried out.
3. Spring-back compensation can be done either in dies or punches and can be validated by numerical simulations.
4. Bauschinger effect can be studied experimentally and can be incorporated in the numerical simulation.

REFERENCES

1. M. Samuel; 13 June 2000, Department of Production Engineering and Machine Design, Faculty of Engineering, Mansoura university, 35516 Mansoura, Egypt.

2. Hongsheng Liu; ZhongwenXing; ZhenzhongSun;JunBao, Engineering Analysis with Boundary Elements 35 (2011) 436–451. School of Mechatronics Engineering, Harbin Institute of Technology, 92 West Da-Zhi Road, Harbin 150001, China.

3. Hosford, William F; Caddell, Robert M, 2007,Metal Forming Mechanics and Metallurgy, Cambridge University Press, New York.

4. Marciniak, Z; Duncan, J.L; Hu, S.J, 2002, Mechanics of Sheet Metal Forming, Butterworth Heinemann, London.

5. Kalpakjian ,Serope ;Schmid ,Steven R,2003,Manufacturing Processes For Engineering Materials, Prentice Hall.

6. R Hill, “The Mathematical Theory of Plasticity”, Oxford, London, 1950.

7. Gardiner,F , 1957,The Sring-back of metals ,Transactions of the ASME, **77**,1-9.

8. Gau,Jenn-Terng ,2001, A new model for Spring-back prediction in which the Bauschinger effect is considered, International Journal of Mechanical Sciences,**43,**1813-1812.

9. Johnson, W, 1981, Spring-back after the biaxial elastic-plastic pure bending of rectangular plate- I, International Journal of Mechanical Sciences, **23,**619-630.

10. Ferreira JA, Sun P, Gracio JJ, 2006, Close loop control of a hydraulic press for springback analysis,J Mater Process Technol ,**177**,377–81.

11. Xiang AnYang , FengRuan International Journal of Mechanical Sciences 53 (2011) 399–406 School of Mechanical and Automotive Engineering, South China University of Technology, GuangZhou 510641, China

12. Sun P, Gracio JJ, Ferreira JA, 2006, Control system of a mini hydraulic press for evaluating spring-back in sheet metal forming. J Mater Process Technol, **176,** 55–61.

13. Tekaslan OO, S_eker U, Ozdemir A, 2006, Determining spring-back amount of steel sheet metal has 0.5 mm thickness in bending dies. Mater Design, **27,**251–8.

14. Dae-Kwei Leu,1997,A Simplified Approach for evaluating Bendability and spring-back in Plastic Bending of Anisotropic Sheets, Journal Of Material Processing Technology , 2006,**66,**9-17.

15. Wang, Chanto et al,1993,Mathematical Modeling of Plain Strain bending of sheet and plate, Journal of material processing technology,**39,**279-304.

16. Li X, Yang Y, Wang Y, Bao J, Shunping L, 2002, Effect of the material-hardening mode on the spring-back simulation accuracy of V-free bending, J Mater Process Technol,**123,**209–11.

17. Rosochwski, 2001, Die compensation procedure to negate die deflection and component spring-back, Journal of Materials Processing Technology, **115**, 187-191.

18. Ayers, R.A, 1984, SHAPESET: A process to reduce sidewall curl spring-back in high strength steel rails, Journal of Applied Metalworking, **3**,127.

19. Liu, Y.C., 1988, The effect of restraining force on shape deviations in flanged channels, Journal of Material Technology, **110**, 389.

20. Woo, D.M, et al, 1959, The Engineer, **208**, 135.

21. Wenner, A.L., 1983, on work hardening and spring-back in plane straining draw forming, Journal of Applied Metalworking, **2**,277.

22. Buste, A., 1999, Prediction of strain distribution in aluminum tailor welded blanks, Proceedings of the International Conference, NUMISHEET, 455-460.

23. Raju, D.V, 2002, Effect of Planar anisotropy on spring-back in plain strain bending, M.Tech Thesis, Department of Mechanical Engineering, IIT Delhi.

24. Soni,Vishal,2001,Generation of code for prediction of spring-back in sheet metal bending operation, M Tech Major Project,2001, IIT Delhi

APPENDICES

A.1 Analytical model for prediction of spring-back considering the strain hardening effect and anisotropy

Assumption:

- Since width (w) very large as compared to the thickness(t), the strain in width direction can be neglected and hence plain strain condition prevails
- Neutral axis shift and bauchinger effect is neglected
- Material is elastic plastic i.e. strain hardening is considered
- Anisotropy material is considered.

Let us assume that the specimen is taken such that the width is perpendicular to the rolling direction as shown below:

The Hill's anisotropy yield criterion is expressed as:

$2f(\sigma_{ij})$=F$(\sigma_y - \sigma_z)^2$+ G$(\sigma_z - \sigma_x)^2$+H$(\sigma_x - \sigma_y)^2$+ 2Lτ_{yz}^2+ 2Mτ_{zx}^2+2τ_{xy}^2 (5.1)

Where

F,G,H,L,M,N are anisotropic constants

For σ_y=$\sigma_z = 0$ and ϵ_y=0 , it can be shown that

R_0 = H/G

And

R_{90}= H/F

Where σ_0 = flow stress

$$\bar{\sigma} = \sqrt{\frac{3}{2}}\left(\frac{1+R_0+R_{90}}{(1+R_0)(1+R_{90}+\frac{R_{90}}{R_0})}\right)\sigma_x \quad (5.2)$$

$$\bar{\varepsilon} = \sqrt{\frac{2}{3}}\left(\frac{(1+R_0)(1+R_{90}+\frac{R_{90}}{R_0})}{1+R_0+R_{90}}\right)\varepsilon_x \quad (5.3)$$

Now $\bar{\sigma}$ and $\bar{\varepsilon}$ can be written as

$\bar{\sigma} = C_1.\sigma_x$ (5.4)

$\bar{\varepsilon} = C_2.\varepsilon_x$

Where

$$C_1 = \sqrt{\frac{3}{2}}\left(\frac{1+R_0+R_{90}}{(1+R_0)(1+R_{90}+\frac{R_{90}}{R_0})}\right) \quad (5.5)$$

$$C_2 = \sqrt{\frac{2}{3}}\left(\frac{(1+R_0)(1+R_{90}+\frac{R_{90}}{R_0})}{1+R_0+R_{90}}\right) \quad (5.6)$$

Engineering strain in the plane at distance z from the mid plane

$$e_x = \frac{L-L_0}{L_0}$$

$$= \frac{(r+z)\Theta - r\,\Theta}{r\,\Theta} \quad (5.7)$$

$$= \frac{z}{r}$$

Therefore

True strain, $\varepsilon_x = \ln\left(1+\frac{z}{r}\right)$ (5.8)

$$\varepsilon_x \approx \frac{z}{r}$$

Considering the elastic core up to z_e distance from the mid plane on each side, the strain in the elastic core is given by

$$\varepsilon_{xe} = \frac{\sigma_0}{E'}$$

Where,

$E' = \frac{E}{1-v^2}$, for plane strain condition. And v is the poisson's ration

$$\Rightarrow \frac{z_e}{r} = \frac{\sigma_0}{E'}$$

$$z_e = r.\frac{\sigma_0}{E'} \quad (5.9)$$

The force acting on elemental strip along x-direction is given by

$dF_x = \sigma_x$. w.dz

The bending moment,

$$dM = dF_x\, z = \sigma_x .w.dz$$

Where,

$\sigma_{x} = \frac{\bar{\sigma}}{C_1}$

Considering strain hardening,

$\bar{\sigma} = K.\bar{\varepsilon}^{n}$

$$= K\ (C_2\ .\ \varepsilon_x)^{n}$$

Therefore

$\sigma_{x} = \frac{K.C_2^n}{C_1}.\varepsilon_{x}^{n}$ (5.10)

The total bending moment can be obtained as

M = $\int_0^{t/2} \sigma_x$.w.z.dz + $\int_{-t/2}^{0} \sigma_x$. w.z.dz

= 2.$\int_0^{t/2} \sigma_x$. w .z dz

But

$\sigma_x = \varepsilon_{x.}E'$

= $\frac{Z}{r}$. $E'$for 0≤ z ≤ t/2

And

$\sigma_x \frac{K.c_2^n}{C_2}$.$\varepsilon_x^nforz_e \leq\ z\ \leq t/2$

Therefore,

M = $\frac{2w}{3r}.E'.z_e^3 + \frac{2.K.C_2.w}{C_{1.}r^n(n+2)}\left[\left(\frac{z}{r}\right)^{n+2} - z_e^{n+2}\right]$ (5.11)

After releasing the load, the bending moment becomes zero. The change in bending moment can be calculated as below

$\Delta\sigma_x = \frac{z}{r} - \frac{z}{r'}$

Where r' is the radius of curvature after releasing the bending load

$\Delta\sigma_x = E'\ \Delta\varepsilon_x$

Therefore

$$\Delta M = 2.\int_0^{\frac{t}{2}} \Delta\sigma_x \ .w.z.dz$$

$$= 2.\int_0^{\frac{t}{2}} \left(\frac{1}{\mathrm{r}} - \frac{1}{\mathrm{r}'}\right).\mathrm{w}.E'.z^2 dz$$

$$= \frac{w.E'.t^3}{12}\left(\frac{1}{r} - \frac{1}{r'}\right)$$

Since M – ΔM = 0, after springback

$$\frac{2}{3}\frac{w}{r}.E'.z_e^3 + \frac{2.K.C_2.W}{C_1\ r^n\ .(n+2\ )}\left[\left(\frac{z}{r}\right)^{n+2} - z_e^{n+2}\right] = \frac{w.E'.t^3}{12}\left(\frac{1}{r} - \frac{1}{r'}\right) \qquad (5.12)$$

$$\frac{1}{r} - \frac{1}{r'} = 8.\frac{z_e^3}{rt^3} + \frac{24KC_2^n}{C_1 r^n (n+2)E'}.\left[\frac{\left(\frac{t}{2}\right)^{n+2} - z_e^{n+2}}{t^3}\right] \qquad (5.13)$$

Change in angle due to spring-back = final angle – initial angle

$$= \alpha_f - \alpha_i$$

Change in angle = $\left(\frac{r'}{r} - 1\right).\alpha_i$